

# Two-dimension to three-dimension transition of chiral spin liquid and fractional quantum Hall phases

Xiaofan Wu and Ya-Hui Zhang\*

William H. Miller III Department of Physics and Astronomy, Johns Hopkins University,  
Baltimore, MD 21218, USA

\* yzhan566@jhu.edu

January 26, 2024

## Abstract

There have been lots of interest in two-dimensional (2D) fractional phases with an emergent  $U(1)$  gauge field. However, many experimental realizations are actually in three-dimensional (3D) systems with infinitely stacked 2D layers. Then a natural question arises: starting from the decoupling limit with 2+1d  $U(1)$  gauge field in each layer, how does the gauge field become 3+1d when increasing inter-layer coupling? Here we propose a 2D to 3D transition through condensing inter-layer exciton. The Goldstone mode of the condensation becomes the missing  $a_z$  component in the 3D phase. We applied this transition mechanism in many different systems.

---

## Contents

<b>1</b>	<b>Introduction</b>	<b>2</b>
<b>2</b>	<b>Transition between 2D and 3D <math>U(1)</math> spin liquid</b>	<b>3</b>
<b>3</b>	<b>3+1 d chiral spin liquid</b>	<b>5</b>
3.1	Gapless photon modes in the 3D CSL	7
3.2	Alternative derivation from Higgs mechanism and its equivalence to $a_z = 0$ gauge	8
<b>4</b>	<b>Critical properties of the 2D to 3D transition</b>	<b>10</b>
4.1	correlation in $z$ -direction	14
<b>5</b>	<b>Continuous transition between gapped fracton order and gapless 3D phase</b>	<b>15</b>
5.1	2D iCSM theory	15
5.2	3D iCSM theory: a gapless phase	17
5.3	Critical theory between gapped fracton order and gapless 3D phase	18
<b>6</b>	<b>Conclusion</b>	<b>19</b>
<b>A</b>	<b>Plane-wave solution to the Maxwell equations</b>	<b>20</b>
<b>B</b>	<b>Effective propagators</b>	<b>21</b>
<b>C</b>	<b>Feynman diagram calculation</b>	<b>22</b>
<b>D</b>	<b>Electromagnetic response of the iCSM</b>	<b>27</b>

## 1 Introduction

The study of quantum phase transitions is one of the major focuses in condensed matter physics [1, 2]. Almost all of the well-studied phase transitions are between two phases in the same space-time dimension. In this paper, we are going to consider an unusual class of critical points between a decoupled two-dimensional (2D) phase and a three-dimensional (3D) phase. More specifically, we consider a system with infinitely stacked 2D layers along the  $z$  direction, which is quite common in quasi-two-dimensional materials including high-temperature superconducting cuprates and many quantum spin liquid candidates. In this kind of setup, the inter-layer coupling is usually weak, so one can consider the decoupling limit with an independent 2D quantum phase at each layer. If the 2D phase is a fractional phase such as a quantum spin liquid or a fractional quantum Hall (FQH) phase, the inter-layer coupling is usually irrelevant and the decoupled 2D phases survive to a finite inter-layer coupling until a phase transition happens. In the larger coupling regime, the natural ground state should be a three-dimensional phase with excitations mobile in the whole 3D space. The focus of this paper is to describe this kind of 2D to 3D transition.

We will consider the case that the decoupled 2D phase has a  $U(1)$  gauge field. Let us take  $U(1)$  spin liquid as examples. In the decoupled phase, both the spinon and the emergent photon are confined in each 2D plane. Upon increasing the inter-layer coupling, one can imagine a 3D phase with both spinon and photon moving in the 3D space. Across this 2D to 3D transition, the spinon should get mobile along the  $z$ -direction, and simultaneously the  $U(1)$  gauge field should acquire a missing  $a_z$  component with additional Maxwell terms. We will show that both can be accomplished simultaneously through condensing an inter-layer exciton formed by a pair of gauge charges (for example, spinon pairs in spin liquid). Such an exciton condensation  $\langle \Phi \rangle \neq 0$  provides a hopping along the  $z$ -direction for the spinon. Besides, the Goldstone mode of the condensation becomes the missing  $a_z$  component of the 3D  $U(1)$  gauge field while its phase stiffness provides the missing Maxwell term.

Following this picture, we propose a continuous critical theory for the 2D to 3D transition of a  $U(1)$  spin liquid. As a simple illustration, we restrict to the simple chiral spin liquid (CSL) as an example. Chiral spin liquids [3, 4] have been found to be the ground state for various spin 1/2 lattice models [5–17] and also in  $SU(N)$  model with  $N > 2$  [18–25]. In the simple  $SU(2)$  case, it can be thought as a Laughlin state [26] of the spin flips. It is by now well established that the low energy theory describing a CSL or a Laughlin state is through Chern-Simons theory of 2+1d  $U(1)$  gauge field [27]. Now we consider a 3D system with infinitely stacked spin layers. When the inter-layer coupling  $J_\perp$  is zero, we assume each layer hosts a chiral spin liquid phase. Then we gradually increase  $J_\perp$  until a phase transition happens. A natural phase transition is through generating the term  $\sum_z \Phi_i(z) f_{i;\sigma}^\dagger(z+1) f_{i;\sigma}(z)$  where  $f_{i;\sigma}(z)$  is the spinon in the layer  $z$ . After the onset of  $\Phi$ , we have a 3+1d  $U(1)$  gauge field, but still with a Chern-Simons term at each layer. This unusual 3D chiral spin liquid turns out to host one gapless mode with quadratic dispersion  $\omega \sim q_z^2$  along the  $z$  direction and linear dispersion along the  $q_x, q_y$  plane.

Next, we study the critical point between the 2D CSL and the gapless 3D CSL. In the small  $J_\perp$  side, the  $z$  coordinate should have scaling dimension  $[z] = 0$  compared to  $x, y, t$ . In contrast, in the large  $J_\perp$  side, we have  $[z] = -\frac{1}{2}$  given the  $\omega \sim q_z^2$  dispersion. Across the

44 quantum critical point (QCP), the scaling dimension of the  $z$  coordinate needs to jump from 0  
 45 to  $-1/2$ . We will show that it remains zero exactly at the QCP. If we fix  $q_x = q_y = 0$ , there is  
 46 gapless mode at every  $q_z \in [0, 2\pi]$ , coming from the critical boson at each layer. The photon  
 47 and other order parameters actually acquire a  $q_z$  dependence, which leads to a finite but non-  
 48 zero correlation length along the  $z$  direction, indicating a more non-trivial structure than a  
 49 trivial decoupled fixed point. More specifically,  $O^{z_1}(x_1)O^{z_2}(x_2) \sim g_O(z_1 - z_2) \frac{1}{|x_1 - x_2|^{a_O}}$ , where  
 50  $x$  denotes the position vector in the  $(t, x, y)$  space. For a decoupled fixed point, we expect  
 51  $g_O(z_1 - z_2) \sim \delta_{z_1, z_2}$ . In contrast, our critical theory has  $g_O(z_1 - z_2) = e^{-\frac{|z_1 - z_2|}{\xi_O}}$ , so an operator  
 52 in one layer correlates with an operator in a layer far away.

53 Although we focus on the CSL, our theory can be easily generalized to infinitely stacked  
 54 quantum Hall layers, given the equivalence between the CSL phase and a bosonic Laughlin  
 55 state. The same construction can lead to a three-dimensional gapless quantum Hall phase.  
 56 Such a state has been discussed in Ref. [28] from a different construction. Our approach then  
 57 provides a continuous critical theory between the 3D quantum Hall phases and the decoupled  
 58 Laughlin states. More recently there have also been discussions of infinite component Chern-  
 59 Simons-Maxwell (iCSM) theory with both intra-layer and inter-layer chern-simons (CS) terms,  
 60 with the motivation to construct fracton phases [29–31]. The  $U(1)$  gauge field in these phases  
 61 is still  $2 + 1$  d without the  $a_z$  component. The inter-layer correlation is encoded through the  
 62 off-diagonal Chern-Simons term. In contrast, in our construction, the inter-layer correlation  
 63 is from a Higgs term, which leads to  $3 + 1$  d  $U(1)$  gauge field. It is then natural to explore the  
 64 case with both inter-layer CS term and inter-layer Higgs condensation. We find that adding  
 65 a Higgs term from inter-layer exciton condensation to the infinite component Chern-Simons  
 66 theory always leads to a 3D gapless phase whose low energy spectrum is quite similar to the  
 67 simple 3D CSL constructed above. Then we can construct a critical theory between a gapped  
 68 fracton phase [32, 33] described by a iCSM theory and a gapless 3D phase. The critical theory  
 69 is very similar to the QCP between the 2D CSL and the 3D CSL. We note that criticality out of  
 70 a fracton phase has also been studied by Ref. [34].

## 71 2 Transition between 2D and 3D $U(1)$ spin liquid

72 In this section, we offer a general framework for the 2D to 3D transition of a  $U(1)$  spin liquid.  
 73 We consider the following multi-layer spin model:

$$H = \sum_z \sum_{\langle ij \rangle} J_{ij} \vec{S}_i(z) \cdot \vec{S}_j(z) + \dots + \sum_z \sum_i J_{\perp} \vec{S}_i(z) \cdot \vec{S}_i(z+1) \quad (1)$$

74 where  $z = 0, 1, 2, \dots, N - 1$  is the coordinate at the  $z$  direction,  $N$  is the number of layers that  
 75 will be taken to infinite,  $i, j$  are the site indices within each layer,  $J_{\perp}$  is the inter-layer coupling.  
 76 In ... we include intra-layer terms such as ring exchange terms or chirality terms, which are  
 77 needed to stabilize a spin liquid phase. As much of this paper is devoted to low-energy field  
 78 theory, the exact form of the microscopic lattice models is not our focus. Throughout this  
 79 paper, we assume there is translation invariance along the  $z$  direction.

80 When  $J_{\perp} = 0$ , we have decoupled 2D layers. We assume that the ground state is a  $U(1)$   
 81 spin liquid with emergent  $2 + 1$  d  $U(1)$  gauge field  $a_{\mu}(t, x, y; z)$ ,  $\mu = 0, x, y$  for each layer  
 82  $z = 0, 1, \dots, N - 1$ . Here the gauge fields in different layers are completely independent. Such  
 83 a spin liquid phase can be conveniently described by the Abrikosov fermion construction [27]:

$$\vec{S}_i(z) = \frac{1}{2} f_{i;\sigma}^{\dagger}(z) \vec{\sigma}_{\sigma\sigma'} f_{i;\sigma'}(z) \quad (2)$$

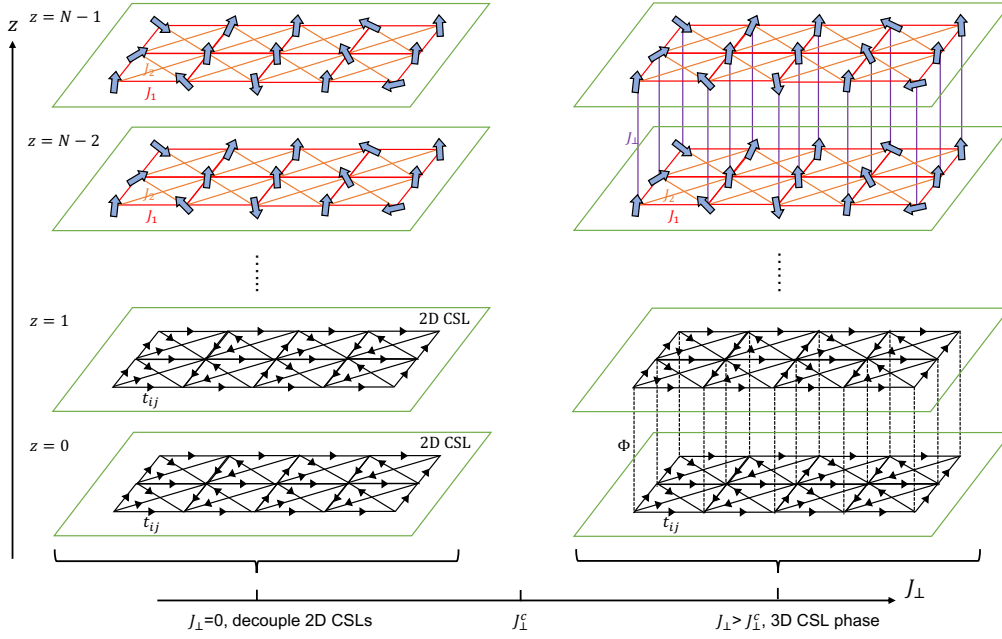


Figure 1: The system we study consists of  $N$  identical layers of spin models or quantum Hall layers. We will take  $N$  to be infinite in the end. In the example considered in this figure, every layer hosts an independent chiral spin liquid (CSL) at the decoupled limit ( $J_{\perp} = 0$ ). When  $J_{\perp} > J_{\perp}^c$ , the inter-layer condensate  $\Phi \neq 0$  generates a hopping term of the spinons between adjacent layers and leads to a new gapless 3D phase with  $3 + 1d$   $U(1)$  gauge field.

84 with the constraint  $\sum_{\sigma=\uparrow,\downarrow} f_{i;\sigma}^{\dagger}(z) f_{i;\sigma}(z) = 1$  for every  $i$  and  $z$ . There is an emergent  $U(1)$   
 85 gauge field  $a_{\mu}$  associated with the gauge symmetry:  $f_{i;\sigma}(z) \rightarrow f_{i;\sigma}(z) e^{i a_{\mu}(z)}$ .

86 Let us start from the decoupled phase:

$$\mathcal{L} = \sum_z \mathcal{L}_z[f(z), a(z)] \quad (3)$$

87 where  $z$  is the layer index and  $a(z)$  is a  $2 + 1$  d gauge field in layer  $z$ .  $\mathcal{L}_z[f(z), a(z)]$  is the  
 88 effective action at each layer  $z$  which we will specify later. At the decoupling limit  $J_{\perp} \rightarrow 0$ ,  $a_{\mu}(z)$   
 89 at different layers fluctuate separately. If we treat the layer index  $z$  as the fourth coordinate,  
 90 we have  $a_{\mu}(x, y, z)$ , with  $\mu = 0, x, y$ . However, there are two essential differences from a true  
 91  $3 + 1$  d gauge field: (I) There is no component  $a_z(x, y, z)$ , which means  $b_y$  and  $b_x$  cannot be  
 92 defined<sup>1</sup>. (II) There is only one polarization mode. In the following, we will show that these  
 93 two problems disappear if we introduce inter-layer exciton condensation.

94 Suppose there is an onset of an inter-layer exciton condensation  $\Phi$  at a critical value of  
 95  $J_{\perp}^c$ . When  $J_{\perp} > J_{\perp}^c$ , spinons between adjacent layers develop a particle-hole pairing term:  
 96  $\Phi(z)_i e^{i \theta_i(z)} \sim \langle f_{i;\sigma}^{\dagger}(z) f_{i;\sigma}(z+1) \rangle \neq 0$ . Here  $\theta_i(z)$  is the phase of the condensation. The mean-  
 97 field Hamiltonian now has a new inter-layer hopping term:

$$H_{\text{inter}} = \sum_z \sum_i \Phi_i(z) e^{i \theta_i(z)} f_{i;\sigma}^{\dagger}(z+1) f_{i;\sigma}(z) + \text{h.c.} \quad (4)$$

98 Next, we want to learn how the effective low-energy theory changes. In the decoupled the-  
 99 ory of each layer, we have gauge transformation:  $f_z \rightarrow f_z e^{i \chi_z(t, x, y)}$ ,  $a_{\mu}^z \rightarrow a_{\mu}^z + \partial_{\mu} \chi_z(t, x, y)$ ,

<sup>1</sup>In continuum theory,  $b_y = \partial_z a_x - \partial_x a_z$ . If the  $a_z$  component is missing,  $b_y$  has no gauge independent definition.

100 where  $t$  comes from the path integral construction and the microscopic lattice points are re-  
 101 placed by continuous coordinates  $x, y$ . Now we have a new condensate field  $\Phi_i(z)e^{i\theta_z}$ , whose  
 102 phase should transform as  $\theta_z \rightarrow \theta_z + \chi_{z+1} - \chi_z$ . From this gauge transformation, we can  
 103 write down the simplest allowed action term for  $\theta$  similar to the standard effective theory of  
 104 a superfluid:

$$S_{\text{int}} = \frac{\rho_s}{2} \int d^3x \sum_z (\partial_\mu \theta_z - (a_\mu^{z+1} - a_\mu^z))^2, \quad (5)$$

105 and it becomes  $f_{\mu 3} f_{\mu 3}$  term in the continuum limit if we see  $\theta$  as the fourth component of the  
 106 vector field  $a_z$  ( $a_z = \theta_z/b$ ,  $b$  is the inter-layer distance):

$$S_{\text{int}} = \frac{\tilde{\rho}_s}{2b} \int d^4x \sum_{\mu=x,y,z} (\partial_\mu a_z - \partial_z a_\mu)^2. \quad (6)$$

107 The coupling of  $\Phi$  to  $f$  is in the form  $\Phi_i(z)e^{ia_z} f_i^\dagger(z+1)f_i(z)$ , exactly as expected for  $a_z$   
 108 component of a U(1) gauge field. Thus we obtain a 3 + 1 d U(1) gauge theory when  $\Phi_z$   
 109 condenses.

110 This transition near  $J_\perp = J_\perp^c$  can be described by the onset of the condensation  $\Phi$ :

$$S = \int d^3x \sum_z \left\{ \sum_{\mu=0,x,y} |(\partial_\mu - i(a_\mu^{z+1} - a_\mu^z))\Phi_z|^2 \right. \\ \left. + r|\Phi_z|^2 + \lambda|\Phi_z|^4 + (\Phi_z f_{z+1;\sigma}^* f_{z;\sigma} + \text{h.c.}) \right\} + \sum_z S_f[f_z, a^z], \quad (7)$$

111 where we assume translation symmetry in the  $z$  direction and  $\int d^3x$  is integrating over  
 112 the  $t, x, y$  space.  $S_f[f_i, a^i]$  is the action of the spinon and gauge field in a single layer, which  
 113 depends on the ansatz and the type of the spin liquid. The reflection symmetry  $R_z : z \rightarrow -z$   
 114 combined with translation  $T_z$  maps  $\Phi_i$  to  $\Phi_i^\dagger$ . So there is an effective particle-hole symmetry for  
 115  $\Phi$ , which forbids the linear  $\partial_\tau$  term in the action. When  $r < 0$ ,  $\Phi_i$  condenses and the decoupled  
 116 2 + 1 d U(1) gauge fields develop the fourth component and transits to a 3 + 1 d U(1) gauge  
 117 field as described above.

118 The above framework works for any U(1) spin liquid no matter whether the spinon is  
 119 gapped or gapless. In the following sections, we apply it to chiral spin liquid, the simplest 2D  
 120 spin liquid with a deconfined U(1) gauge field but with gapped matter. In Sec. 3 we constructs  
 121 a 3+1d CSL following this approach. The critical theory of the 2D to 3D transition of the CSL is  
 122 discussed in Sec. 4. In Sec. 5 we generalize our theory to an infinite component Chern-Simons  
 123 theory with inter-layer Chern-Simons terms which may describe a fracton phase. Sec. 6 is the  
 124 conclusion.

### 125 3 3+1 d chiral spin liquid

126 In this section, we study the new 3 + 1d CSL phase after the condensation transition. To begin  
 127 with, here we give a brief introduction to CSL in a single 2D layer. From a spin-1/2 model,  
 128 using the Abrikosov fermion construction in Eq. 2, we can write down a spinon mean-field  
 129 ansatz for the CSL phase:

$$H_{\text{mean}} = \sum_{\langle ij \rangle} -\frac{1}{2} J_{ij} [(f_{i\sigma}^\dagger f_{j\sigma} t_{ji} + \text{h.c.}) - |t_{ij}|^2] + \sum_i a_0(i) (f_{i\sigma}^\dagger f_{i\sigma} - 1). \quad (8)$$

130 Here  $t_{ij}$  is the spinon pairing which satisfies the self-consistency equation

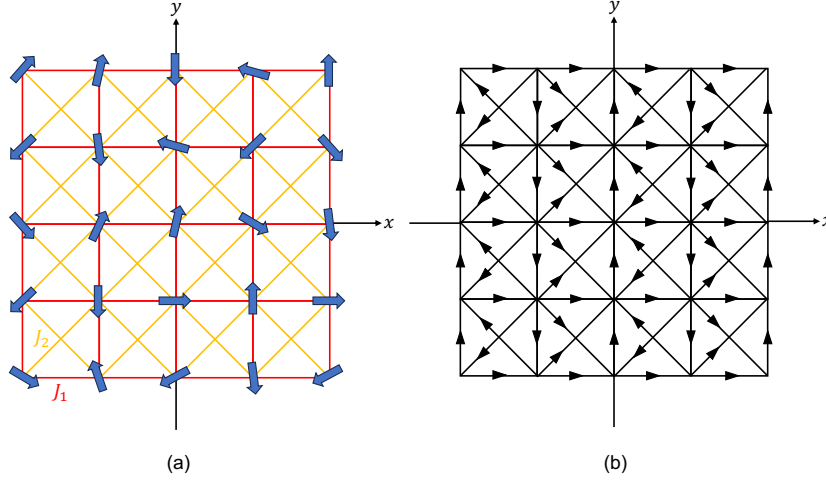


Figure 2: (a) The frustrated Heisenberg model of spin-1/2 on the square lattice.  $J_1$  and  $J_2$  are the nearest and the second nearest coupling constants. (b) The mean-field ansatz of CSL. The hopping  $t_{ij}$  has a  $\frac{\pi}{2}$  phase in the direction of the arrow. This mean-field ansatz induces  $\pi$  flux for each square and  $\frac{\pi}{2}$  flux for each triangle.

$$t_{ij} = \langle f_{i\sigma}^\dagger f_{j\sigma} \rangle, \quad (9)$$

131 and  $a_0(i)$  is determined by the constraint

$$\langle f_{i\sigma}^\dagger f_{i\sigma} \rangle = 1 \quad (10)$$

132 at each site. These self-consistent equations may have different solutions of  $t_{ij}$  and we call  
 133 these solutions the mean-field ansatzes. Fig. 2(b) is an example, where we have  $t_{i,i+x} = it_1$ ,  
 134  $t_{i,i+y} = it_1(-1)^{i_x}$ ,  $t_{i,i+x+y} = t_{i,i+x-y} = -it_2(-1)^{i_x}$ ,  $a_0(i) = 0$ . Next, we consider the fluctua-  
 135 tions around the mean field. Since the amplitude fluctuation of  $t_{ij}$  is gapped, we only consider  
 136 its phase fluctuation  $t_{ij}e^{ia_{ij}}$ . We also need to include the fluctuation of  $a_0$  since in the path in-  
 137 tegral formalism it gives the exact constraint Eq. 10. Then we can write down the path integral  
 138 of the system:

$$Z = \int \mathcal{D}f \mathcal{D}[a_0(i)] \mathcal{D}a_{ij} e^{i \int dt L}, \quad (11)$$

$$L = \sum_i f_{i\sigma}^\dagger i \partial_t f_{i\sigma} - \left( \sum_{\langle ij \rangle} -\frac{1}{2} J_{ij} [(f_{i\sigma}^\dagger f_{j\sigma} t_{ji} e^{ia_{ji}} + \text{h.c.}) - |t_{ij}|^2] + \sum_i a_0(i) (f_{i\sigma}^\dagger f_{i\sigma} - 1) \right).$$

139 The fluctuations described by  $a_0$  and  $a_{ij}$  are actually a U(1) gauge theory. From the  
 140 Abrikosov fermion construction Eq. 2, we see there is a gauge transformation

$$\begin{aligned} f_{i\sigma} &\rightarrow f_{i\sigma} e^{i\chi_i}, \\ f_{i\sigma}^\dagger &\rightarrow f_{i\sigma}^\dagger e^{-i\chi_i}, \\ a_{ij} &\rightarrow a_{ij} + \chi_j - \chi_i, \\ a_0 &\rightarrow a_0 + \partial_t \chi_i \end{aligned} \quad (12)$$

141 that does not change the physical state. In Eq. 11,  $a_0$  and  $a_{ij}$  behave like external electromag-  
 142 netic perturbation coupled to the spinon with unit charge. If the ground state is a filled spinon

143 band with a nonzero Chern number, there should be a Hall conductance. Thus we will get the  
 144 following Chern-Simons theory in the continuum limit after integrating out spinon  $f$ :

$$S = \frac{2}{4\pi} \int d^3x \epsilon^{\mu\nu\rho} a_\mu \partial_\nu a_\rho, \quad (13)$$

145 where we assume the Chern number of the filled band is 1 and the factor 2 comes from  $\sigma = \pm$ .  
 146 This can be realized by the CSL mean-field ansatz in Fig. 2(b). This Chern-Simons theory has  
 147 an infinitely large gap. To see this, we can add a very small Maxwell term to the theory (since  
 148 it is irrelevant compared to the Chern-Simons term):

$$S = \frac{2}{4\pi} \int d^3x \epsilon^{\mu\nu\rho} a_\mu \partial_\nu a_\rho - \frac{1}{4g^2} \int d^3x f_{\mu\nu} f^{\mu\nu}. \quad (14)$$

149 Note that Eq. 14 is written in Minkovski space-time. In most sections throughout this paper  
 150 (except for Sec. 3.1) we are using the Euclidean space-time action. So we also write down the  
 151 Euclidean space-time counterpart of Eq. 14 here:

$$S = \frac{2i}{4\pi} \int d^3x \epsilon_{\mu\nu\rho} a_\mu \partial_\nu a_\rho + \frac{1}{4g^2} \int d^3x (\partial_\mu a_\nu - \partial_\nu a_\mu)^2, \quad (15)$$

152 where  $\mu, \nu, \rho$  are summed over 0, 1, 2,  $\epsilon^{012} = -\epsilon_{012} = 1$ .

153 By solving the equation of motion, we get a single photon mode with an energy gap

$$E_{\text{gap}} = \frac{g^2}{\pi}, \quad (16)$$

154 which goes to infinity in the limit  $g^2 \rightarrow \infty$ .

155 Next, we turn on the interlayer coupling  $J_\perp$  and let the system go through the transition.  
 156 Now we have a new phase variable  $\theta$  of the condensate  $\Phi$  to be the  $a_z$  component. As we shall  
 157 see, a new gapless photon mode shows up in the new 3+1 d CSL.

### 158 3.1 Gapless photon modes in the 3D CSL

159 After the condensation transition, in addition to the mean-field Hamiltonian Eq. 8 for each  
 160 layer, there is a new spinon hopping term in the Hamiltonian which allows the spinon to hop  
 161 between different layers. The mean field Hamiltonian now is:

$$\begin{aligned} H &= H_{\text{mean}} + H_{\text{inter}} \\ &= \sum_z \sum_{\langle ij \rangle} -\frac{1}{2} J_{ij} \left[ (f_{i;\sigma}^\dagger(z) f_{j;\sigma}(z) t_{ji} e^{i a_{ji}(z)} + \text{h.c.}) - |t_{ij}|^2 \right] \\ &\quad + \sum_i a_0^z(i) (f_{i;\sigma}^\dagger(z) f_{i;\sigma}(z) - 1) + \sum_z \sum_i \Phi_i(z) e^{i a_z^z} f_{i;\sigma}^\dagger(z+1) f_{i;\sigma}(z) + \text{h.c.} \end{aligned} \quad (17)$$

162 where  $a_z^z$  is the phase of the condensation  $\Phi_z(z)$ .

163 Integrating out the spinon, we get the low energy effective theory of phase fluctuations:

$$\begin{aligned} S &= \frac{2i}{4\pi} \sum_z \int d^3x \epsilon_{\mu\nu\rho} a_\mu^z \partial_\nu a_\rho^z + \frac{1}{4g^2} \sum_z \int d^3x (\partial_\mu a_\nu^z - \partial_\nu a_\mu^z)^2 \\ &\quad + \frac{\rho_s}{2} \sum_z \int d^3x (\partial_\mu a_z^z - (a_\mu^{z+1} - a_\mu^z))^2. \end{aligned} \quad (18)$$

164 We can take the continuum limit in the  $z$ -direction in the equation above and get a contin-  
 165 uum model of the 3+1 d CSL. Note that under the continuum limit, the second line becomes  
 166 the missing Maxwell term  $(\partial_\mu a_z - \partial_z a_\mu)^2$ . The Minkovski action in the continuum limit is as  
 167 follows:

$$S = \frac{1}{b} \int d^4x \left( -\frac{1}{4g^2} f_{\mu\nu} f^{\mu\nu} - \frac{\tilde{\rho}_s}{2} f_{\mu 3} f^{\mu 3} + \frac{k}{4\pi} \epsilon^{\mu\nu\rho} a_\mu \partial_\nu a_\rho \right), \quad (19)$$

168 where  $b$  is the inter-layer distance,  $k = 2$  is the integer level in Chern-Simons theory,  $\tilde{\rho}_s = \rho_s b^2$ ,  
 169  $\mu, \nu, \rho$  run over 0, 1, 2. The first term is the 2 + 1 d Maxwell term. The coefficient of  $f_{\mu 3} f^{\mu 3}$   
 170 is different from the first term since it is generated by the condensation mechanism. The third  
 171 term is the Chern-Simons term.

172 We can use the variational principle  $\delta S = 0$  to get the classical equation of motion. In  
 173 Maxwell's theory, this gives us the inhomogeneous part of the Maxwell's equations (we do not  
 174 include sources in the action for the moment). The homogeneous part does not change. So  
 175 we have a new set of "Maxwell's equations":

$$\nabla \cdot \vec{e} + (\tilde{\rho}_s g^2 - 1) \partial_z e_z - \frac{k g^2}{2\pi} b_z = 0, \quad (20)$$

$$\partial_t \vec{e} - \nabla \times \vec{b} - (\tilde{\rho}_s g^2 - 1) \partial_z (\hat{z} \times \vec{b}) - \frac{k g^2}{2\pi} \hat{z} \times \vec{e} = 0, \quad (21)$$

$$\nabla \cdot \vec{b} = 0, \quad (22)$$

$$\nabla \times \vec{e} + \partial_t \vec{b} = 0. \quad (23)$$

176 Now we can find the plane wave solutions  $\vec{e} = \mathcal{E} e^{i\mathbf{q}\cdot\mathbf{x} - i\omega t}$ ,  $\vec{b} = \mathcal{B} e^{i\mathbf{q}\cdot\mathbf{x} - i\omega t}$  to the equations  
 177 above. Details are in Appendix. A). We get two photon modes  $\mathcal{B}_\pm$  (we choose to use the  
 178 magnetic field) with dispersion relations

$$\omega_\pm^2 = q_x^2 + q_y^2 + \tilde{\rho}_s g^2 q_z^2 + \frac{k^2 g^4}{8\pi^2} \pm \frac{k^2 g^4}{8\pi^2} \sqrt{1 + \frac{16\pi^2 \tilde{\rho}_s}{k^2 g^2} q_z^2} \quad (24)$$

179 We can see that  $\mathcal{B}_+$  has an energy gap  $\frac{k g^2}{2\pi}$  which goes to infinity as  $g^2 \rightarrow \infty$ , while  $\mathcal{B}_-$   
 180 is a gapless mode with  $\omega_-^2 = q_x^2 + q_y^2 + \frac{4\pi^2 \tilde{\rho}_s^2}{k^2} q_z^4 + \dots$  when  $q_z$  is small.  $\mathcal{B}_\pm$  are elliptically  
 181 polarized with opposite circular direction. In other words, the Chern-Simons term will pick up  
 182 a preferred circular direction. When the wave vector  $\mathbf{q}$  lies in  $x - y$  plane, we can see that  $\mathcal{B}_\pm$   
 183 both become linearly polarized: the gapped mode  $\mathcal{B}_+$  is in  $z$  direction while the new gapless  
 184 mode  $\mathcal{B}_-$  lies in  $x - y$  plane. Remember that in 2+1 d Chern-Simons theory, there is only one  
 185 gapped mode and the magnetic field only has a  $z$ -component. Here  $\mathcal{B}_+$  looks very similar to  
 186 that mode: it is linearly polarized in the  $z$ -direction and has a large energy gap which goes  
 187 to infinity as  $g^2 \rightarrow \infty$  as in 2 + 1 d Chern-Simons theory. The other gapless mode  $\mathcal{B}_-$  lies  
 188 in the  $x$ - $y$  plane, which cannot exist unless we have the fourth component of the gauge field.  
 189 So starting from the 2D CSL, the gapped photon mode remains gapped across the transition,  
 190 while a new gapless mode emerges only after the transition.

### 191 3.2 Alternative derivation from Higgs mechanism and its equivalence to $a_z = 0$ 192 gauge

193 When the number of layers  $N$  is finite, one can treat our theory as purely 2 + 1d. In 2 + 1d  
 194 theory, the phase  $\theta$  of the condensate  $\Phi$  is just like the Goldstone mode in Higgs-mechanism.  
 195 So how do we understand the gapless photon mode in the Higgs language?



196 Instead of treating  $\theta$  as  $a_z$  to get the continuum 3 + 1 d  $U(1)$  gauge theory, we can also  
 197 integrate it out to get a 2 + 1 d  $U(1)$  gauge theory. This approach is essentially the same as  
 198 using the  $a_z = 0$  gauge of the 3 + 1 d gauge field. Integrating out  $\theta$  in Eq.(5) gives a additional  
 199 term  $S_{\text{int}}$ :

$$\begin{aligned} S_{\text{int}} &= \frac{\rho_s}{2} \sum_z \int d^3x \left( a_\mu^{z+1,\perp} - a_\mu^{z,\perp} \right)^2 \\ &= \frac{1}{2} \sum_{q_z} \int \frac{d^3q}{(2\pi)^3} u(q_z) a_\mu^{q_z}(q) \left( \delta_{\mu\nu} - \frac{q_\mu q_\nu}{q^2} \right) a_\nu^{-q_z}(-q), \end{aligned} \quad (25)$$

200 where  $a_\mu^\perp$  is the transverse component of the gauge field satisfying  $\partial_\mu a_\mu^\perp = 0$  [35],  $\mu, \nu = 0, 1, 2$ ,  
 201  $q_z = 0, \frac{2\pi}{N}, \dots, \frac{2\pi(N-1)}{N}$  is the discrete momentum in  $z$ -direction, the coefficient

$$u(q_z) = 4\rho_s \sin^2(q_z/2) \quad (26)$$

202 is  $q_z$  dependent. The subscript ‘‘int’’ stands for inter-layer condensation. The above action is  
 203 just the familiar Higgs mass for  $U(1)$  gauge field which however is  $q_z$  dependent.

204 Then the 3 + 1 d CSL is described by the action

$$\begin{aligned} S &= \frac{ik}{4\pi} \sum_z \int d^3x \epsilon_{\mu\nu\rho} a_\mu^z \partial_\nu a_\rho^z + \frac{1}{4g^2} \sum_z \int d^3x (\partial_\mu a_\nu^z - \partial_\nu a_\mu^z)^2 + S_{\text{int}} \\ &= \frac{1}{2} \sum_{q_z} \int \frac{d^3q}{(2\pi)^3} a_\mu^{q_z}(q) \left[ \frac{k}{2\pi} \epsilon_{\mu\rho\nu} q_\rho + \left( \frac{q^2}{g^2} + u(q_z) \right) \left( \delta_{\mu\nu} - \frac{q_\mu q_\nu}{q^2} \right) \right] a_\nu^{-q_z}(-q) \\ &= \frac{1}{2} \sum_{q_z} \int \frac{d^3q}{(2\pi)^3} a_\mu^{q_z}(q) (D^{-1})_{\mu\nu}^{q_z}(q) a_\nu^{-q_z}(-q). \end{aligned} \quad (27)$$

205 Here we work in imaginary time so the Chern-Simons term is imaginary.  $q = (q_0, q_x, q_y)$  is the  
 206 2+1 d wave vector and  $q^2 = q_0^2 + q_x^2 + q_y^2$ .  $g^2$  is a large coupling constant. We can inverse the  
 207 matrix in the transverse subspace to get the photon propagator:

$$D_{\mu\nu}^{q_z}(q) = \frac{-2\pi/k}{q^2 + \frac{4\pi^2}{k^2} (u(q_z) + \frac{q^2}{g^2})} \epsilon_{\mu\nu\rho} q_\rho + \frac{\frac{4\pi^2}{k^2} (u(q_z) + \frac{q^2}{g^2})}{q^2 + \frac{4\pi^2}{k^2} (u(q_z) + \frac{q^2}{g^2})} \left( \delta_{\mu\nu} - \frac{q_\mu q_\nu}{q^2} \right). \quad (28)$$

208 The dispersion relations are given by its poles,

$$\omega_\pm^2 = \mathbf{q}^2 + g^2 u(q_z) + \frac{k^2 g^4}{8\pi^2} \pm \frac{k^2 g^4}{8\pi^2} \sqrt{1 + \frac{16\pi^2 u(q_z)}{k^2 g^2}}, \quad (29)$$

209 where  $\mathbf{q}^2 = q_x^2 + q_y^2$ . This is the discrete version of Eq.(24). We can see that the  $\omega_+$  mode has  
 210 an energy gap  $\frac{k g^2}{2\pi}$  which goes to infinity as  $g^2 \rightarrow \infty$ , while at small  $q_z$ ,  $\omega_-^2 = \mathbf{q}^2 + \frac{4\pi^2 \rho_s^2 q_z^4}{k^2}$  is  
 211 gapless.

212 If  $N$  is finite, then  $q_z = \frac{2\pi}{N} j, j = 0, 1, \dots, N-1$  is discrete. Then we find that only the  
 213  $q_z = 0$  mode is gapless while the other modes are all gapped. This is in agreement with our  
 214 expectations. Considering a 2D system with  $N$  number of layers, condensation of  $\Phi$  just locks  
 215 the  $U(1)$  gauge fields from different layers together, while other components acquire a mass  
 216 term. However, when  $N$  approaches infinite, the gap of other components decreases as  $\frac{1}{\sqrt{N}}$  and  
 217 we need to view the system as 3D above this small energy scale.

## 218 4 Critical properties of the 2D to 3D transition

219 In the last section, we discussed the properties of the 3D CSL phase after the condensation  
 220 transition. In this section, we are going to discuss the critical point at  $J_{\perp} = J_{\perp}^c$ . In Eq. 7, when  
 221 the spinon fulfills the ansatz for CSL (see Fig. 2), we can integrate out the spinon field and get  
 222 the following action:

$$S = \sum_z \int d^3x |(\partial_{\mu} - i(a_{\mu}^{z+1} - a_{\mu}^z))\Phi_z|^2 + \frac{i\alpha}{4\pi} \sum_z \int d^3x \epsilon_{\mu\nu\rho} a_{\mu}^z \partial_{\nu} a_{\rho}^z + s|\Phi|^2 + \frac{1}{2} \sum_{z,z'} \lambda_{z,z'} \int d^3x |\Phi_z|^2 |\Phi_{z'}|^2. \quad (30)$$

223 Here  $\Phi_z$  is a complex boson between layer  $z$  and  $z + 1$ ,  $\alpha = 2$  since we have spin  $\sigma = \uparrow, \downarrow$ .  
 224 In the  $|\Phi|^4$  term we assume  $\lambda_{z,z'}$  has translational symmetry along the  $z$  direction. Note that  
 225 we have a critical boson  $\Phi_z$  at each layer  $z$  and the gauge field in the action is  $2 + 1d$ . We  
 226 list the gauge invariant physical operators at both the critical point and the 3D CSL phase in  
 227 Table.(1). We can see that the new field strength  $b_3, e_1, e_2$  in the 3D phase developed from  
 228 the current operator related to the phase of  $\Phi$  at the critical point. When  $s > 0$ , this mode is  
 229 gapped. When  $s < 0$ , the phase of  $\Phi$  becomes the gapless photon mode in the 3D phase.

230 We note that the gauge symmetry forbids  $\Phi_z^{\dagger} \Phi_{z+1}$  term, so the critical bosons  $\Phi_z$  from  
 231 different layers do not hybridize. However, the Higgs boson at one layer can interact with  
 232 the boson at another layer through the photon  $a_{\mu}$ . Although the  $U(1)$  gauge field  $a_{\mu}$  is still  
 233  $2 + 1d$  in the sense that there is only  $\mu = 0, x, y$  component, we will see that the photon  
 234 acquires a  $q_z$  dependence. But the  $q_z$  dependence is not through the usual dispersion: the  
 235 photon energy is zero for any  $q_z$  as long as  $\mathbf{q} = 0$ . In the following, we use  $\mathbf{q}$  to indicate the  
 236 momentum in the  $x, y$  plane. In the end, our critical theory has infinite gapless critical modes  
 237 coming from the layer structure, but it is not in a trivial layer decoupled fixed point. More  
 238 specifically, the correlation function has the form  $O^{z_1}(x_1)O^{z_2}(x_2) \sim g_O(z_1 - z_2) \frac{1}{|x_1 - x_2|^{\alpha_O}}$ , where  
 239  $x$  denotes the coordinate vector in the  $(t, x, y)$  plane. For a decoupled fixed point, we expect  
 240  $g_O(z_1 - z_2) \sim \delta_{z_1, z_2}$ . In contrast, our critical theory has  $g_O(z_1 - z_2) = e^{-\frac{|z_1 - z_2|}{\xi_O}}$ . When  $s < 0$ ,  
 241 the  $z$  coordinate becomes normal and we can take the continuum limit. However, at  $s = 0$  we  
 242 need to maintain the layer structure in the theory and keep the modes from each  $q_z \in [0, 2\pi)$ .

243 In order to do controlled perturbative calculation, we use the large  $N_b$  expansion [36] to  
 244 study the critical behavior at the transition point. We assume there are  $N_b$  flavors of bosonic  
 245 fields  $\Phi_z^a$  at each layer, which also means that we have  $N_b$  flavors of spinon since  $\Phi$  represents  
 246 spinon pairing so we should make substitution  $\alpha \rightarrow N_b \alpha$  in the Chern-Simons term. The action  
 247 now becomes:

$$S = \sum_z \sum_{a=1}^{N_b} \int d^3x |(\partial_{\mu} - i(a_{\mu}^{z+1} - a_{\mu}^z))\Phi_z^a|^2 + \frac{iN_b\alpha}{4\pi} \sum_z \int d^3x \epsilon_{\mu\nu\rho} a_{\mu}^z \partial_{\nu} a_{\rho}^z + \frac{1}{2} \sum_{z,z'} \sum_{a,b=1}^{N_b} \int d^3x \lambda_{z,z'} |\Phi_z^a|^2 |\Phi_{z'}^b|^2. \quad (31)$$

248 In many circumstances, the Chern-Simons term has been shown to have no RG flowing up  
 249 to two-loop level [37, 38]. So it is a good guess to assume  $\alpha = 2$  in this action. The mass term  
 250 for  $\Phi$  is tuned to be zero. In addition, in writing down the quartic  $\Phi^4$  term, we have assumed  
 251 the  $SU(N_b)$  symmetry at each layer is preserved at the critical point.  $\lambda_{z,z'}$ , which is empirically  
 252 of order  $1/N_b$ , may have a specific form but should have translational invariance. Its exact

Operators at the critical point		Operators in the 3D phase
$ \Phi_z ^2 \sim \vec{S}_i(z) \cdot \vec{S}_i(z+1)$		
$\partial_\mu a_\nu - \partial_\nu a_\mu \sim b_3, e_1, e_2$	$\iff$	$\partial_\mu a_\nu - \partial_\nu a_\mu \sim b_3, e_1, e_2$
$2\text{Im} \left\{ \Phi_z^* \left( \partial_\mu - i \left( a_\mu^{z+1} - a_\mu^z \right) \right) \Phi_z \right\}$ $\sim \text{Current } J_\mu$	$\iff$	$\partial_\mu a_z - \partial_z a_\mu \sim b_1, b_2, e_3$

Table 1: Physical quantities and their associated operators at both the critical point and the 3D phase.

253 form, as we will see, is not important as long as the first order correction is concerned. The  
254 bare photon propagator is (throughout this paper, we use the Landau gauge<sup>2</sup>)

$$D_{0,\mu\nu}^{z,z'}(q) = -\frac{2\pi}{N_b \alpha} \frac{\epsilon_{\mu\nu\lambda} q_\lambda}{q^2} \delta^{z,z'} = D_{0,\mu\nu}(q) \delta^{z,z'}. \quad (32)$$

255 We introduce a new field variable  $\alpha_\mu^z = a_\mu^{z+1} - a_\mu^z$  and use it in the Feynman diagram  
256 calculation. We may also call it photon in the following. Its bare propagator is

$$\tilde{D}_{0,\mu\nu}^{z,z'}(q) = D_{0,\mu\nu}(q) (2\delta^{z,z'} - \delta^{z,z'+1} - \delta^{z,z'-1}). \quad (33)$$

257 Finally, we do a Hubbard-Stratonovich (HS) transformation and introduce a bosonic field  
258  $\varphi_z$  to decompose the  $\Phi^4$  term. The action is given below, where we leave the quadratic parts  
259 of  $\varphi$  and  $\alpha$  since we are to use their large  $N_b$  effective propagators in the Feynman diagram  
260 calculation.

$$S = \sum_z \sum_{a=1}^{N_b} \int d^3x |(\partial_\mu - i\alpha_\mu^z) \Phi_z^a|^2 + \sum_z \sum_{a=1}^{N_b} \int d^3x \varphi_z |\Phi_z^a|^2. \quad (34)$$

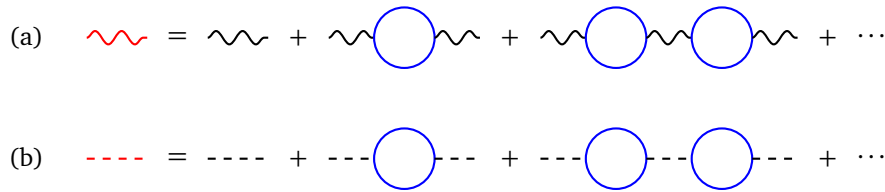


Figure 3: Bubble diagrams for the effective propagators of the gauge field and the HS field  $\varphi$ . The bare propagators are of order  $1/N_b$  and each boson loop (blue circle) has a factor of  $N_b$ , so all the bubble diagrams are of the same order  $1/N_b$ . (a) Black wavy lines represent the bare photon propagator  $\tilde{D}_0$  (Eq. 32 and Eq. 33). The red wavy line represents the effective photon propagator  $\tilde{D}_{\text{eff}}$ . (b) Black dashed lines represent the bare propagator  $G_{\varphi,0}^{z,z'} = -\lambda_{z,z'}$ . The red dashed line represents the effective propagator  $G_{\varphi,\text{eff}}$ .

261 In Appendix. B we present the calculation of the effective propagators of the gauge field  
262 and the scalar  $\varphi$ . Due to the translational invariance in  $z$ -direction, we can Fourier transform

<sup>2</sup>This can be done by adding a gauge fixing term  $(1/2\xi)(\partial_\mu \alpha_\mu^z)^2$  to get rid of the zero eigen-value problem when doing the matrix inverse, and then take the limit  $\xi \rightarrow 0$  in the resulting propagator.

263 the layer index into  $q_z$ . In the following we use  $q_\mu, p_\mu$  for the momentum in the  $(0, x, y)$   
 264 subspace.  $q_z$  is used as an additional index. The propagators for the gauge field  $\alpha$  and the  
 265 scalar  $\varphi$  are

$$\tilde{D}_{\text{eff},\mu\nu}^{q_z}(q) = \frac{A(q_z)}{N_b} \left( \frac{B(q_z)}{|q|} \left( \delta_{\mu\nu} - \frac{q_\mu q_\nu}{q^2} \right) - \frac{\epsilon_{\mu\nu\lambda} q_\lambda}{q^2} \right) + \mathcal{O}(1/N_b^2), \quad (35)$$

266

$$G_{\varphi,\text{eff}}^{q_z}(p) = -\frac{8|p|}{N_b} + \mathcal{O}(1/N_b^2), \quad (36)$$

267 where we introduced two  $q_z$  dependent functions  $A(q_z)$  and  $B(q_z)$  as follows:

$$A(q_z) = \frac{8\pi \sin^2 \frac{q_z}{2}}{1 + \frac{\pi^2 \sin^4 \frac{q_z}{2}}{4\alpha^2}}, \quad B(q_z) = \frac{\pi \sin^2 \frac{q_z}{2}}{2\alpha}. \quad (37)$$

268 We can also get the propagator of the original gauge field  $a_\mu$  using:

$$D_{\text{eff},\mu\nu}^{q_z}(q) = \frac{\tilde{D}_{\text{eff},\mu\nu}^{q_z}(q)}{4 \sin^2 \frac{q_z}{2}}, \quad (38)$$

269 which also shows  $q_z$  dependence. This is because the condensate field  $\Phi_z$  couples to  $a_\mu^{z+1} - a_\mu^z$   
 270 and therefore the bubble diagrams Fig. 3 connect  $a_\mu$  at different layers.

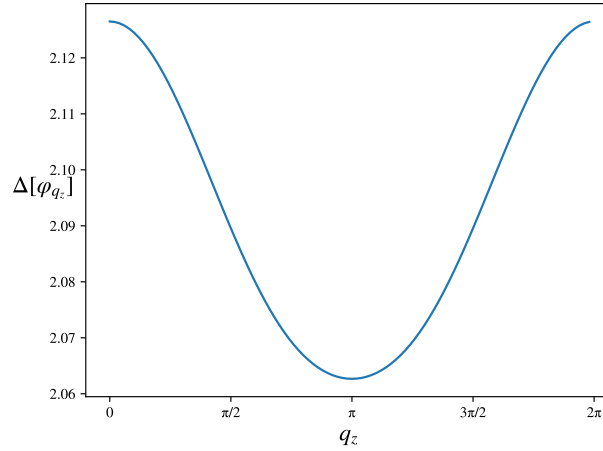


Figure 4: Scaling dimension of  $\varphi_{q_z}$  given by Eq. 40 and Eq. 41. We choose  $N_b = 2$ ,  $\alpha = 2$ , and take  $N \rightarrow \infty$  so the momentum summation is replaced by an integral.

271 On the contrary, there is no  $q_z$  dependence in the leading order for  $\varphi$ . This is because  $\varphi_z$   
 272 couples to  $|\Phi_z^a|^2$  and the bubble diagrams in Fig. 3 only connect  $\varphi_z$  at the same layer. So the  
 273 effective propagator  $G_{\varphi,\text{eff}}^{q_z}$  is  $q_z$  independent. However,  $G_\varphi$  will still acquire a  $q_z$  dependence  
 274 in the next order of  $1/N_b$ .

275 We calculate the scaling dimension of  $\varphi$  up to order  $1/N_b$  using the same techniques in  
 276 Ref. [36]. Basically, we calculate the logarithmic divergent part of the 2-point correlation  
 277 function  $\langle \varphi_z(x) \varphi_{z'}(0) \rangle$  and then reexponentiate it. The results are summarized in Table. 2  
 278 and the detailed calculation is in Appendix. C. It turns out that the scaling dimensions of  $\varphi_z$  at  
 279 each layer are mixed and we need to go to the  $q_z$  space and find out the independent scaling  
 280 dimensions of the operators  $\varphi_{q_z}(x) = \frac{1}{\sqrt{N}} \sum_z e^{-iq_z \cdot z} \varphi_z(x)$ . Then we sum over the results in  
 281 Table. 2, Fourier transform it into  $q_z$  space, and reexponentiate it. Finally we obtain the 2-  
 282 point correlation function


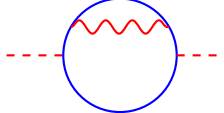
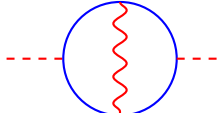
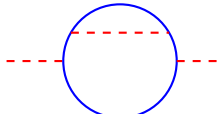
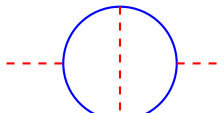
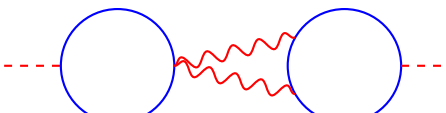
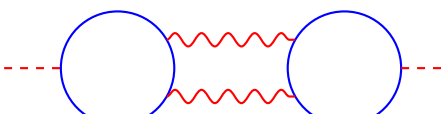
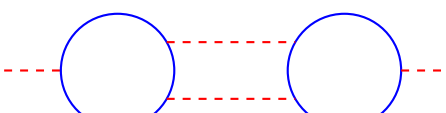
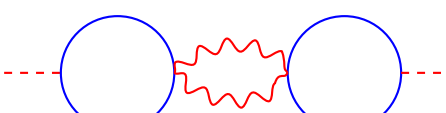
A.		$= \frac{8}{\pi^2 N_b  x ^4} \delta_{z,z'} = U \delta_{z,z'}$
B.		$= -2 \times \frac{2}{3\pi^2 N_b} \cdot \frac{1}{N} \sum_{q_z} A(q_z) B(q_z) \ln(x^2 \Lambda^2) U \delta_{z,z'}$
C.		$= 0$
D.		$= 2 \times \frac{2}{3\pi^2 N_b} \ln(x^2 \Lambda^2) U \delta_{z,z'}$
E.		$= \frac{4}{\pi^2 N_b} \ln(x^2 \Lambda^2) U \delta_{z,z'}$
F.		$= \frac{1}{4\pi^2 N_b} \cdot \frac{1}{N} \sum_{q_z, l_z} e^{iq_z \cdot (z-z')} A(l_z) A(q_z - l_z) \cdot (B(l_z) B(q_z - l_z) - 1) \ln(x^2 \Lambda^2) U$
G.		$= 0$
H.		$= 0$
I.		$= 0$

Table 2: Results for the individual Feynman diagrams appearing in the first order correction to the 2-point correlation function  $\langle \varphi_z(x) \varphi_{z'}(0) \rangle$ . We only calculate the logarithmic divergent part of each diagram and zero means no logarithmic divergence.

$$G_\varphi^{q_z}(x) = \langle \varphi_{q_z}(x) \varphi_{-q_z}(0) \rangle = \left( \frac{8}{\pi^2 N_b |x|^4} \right) \left( \frac{1}{x^2 \Lambda^2} \right)^{\Delta_{q_z}^{(1)}}, \quad (39)$$

283 where  $x = (t, x, y)$ ,  $x^2 = t^2 + x^2 + y^2$ ,  $\Lambda$  is a momentum cutoff,  $\Delta_{q_z}^{(1)}$  is the anomalous  
284 dimension of  $\varphi_{q_z}$  at order  $1/N_b$ ,

$$\begin{aligned} \Delta_{q_z}^{(1)} = & \frac{4}{3\pi^2 N_b} \frac{1}{N} \sum_{l_z} A(l_z) B(l_z) - \frac{16}{3\pi^2 N_b} \\ & - \frac{1}{4\pi^2 N_b} \frac{1}{N} \sum_{l_z} A(l_z) A(q_z - l_z) (B(l_z) B(q_z - l_z) - 1). \end{aligned} \quad (40)$$

285 The scaling dimension of  $\varphi$  is

$$\Delta[\varphi_{q_z}] = 2 + \Delta_{q_z}^{(1)} + \mathcal{O}(1/N_b^2). \quad (41)$$

286 We also show the numerical result of  $\Delta[\varphi_{q_z}]$  for infinite-layer case ( $N \rightarrow \infty$ ) in Fig. 4.

#### 287 4.1 correlation in $z$ -direction

288 Note that  $\varphi$  is a gauge invariant operator, it corresponds to a physical observable

$$|\Phi(z)|^2 \sim \vec{S}_i(z) \cdot \vec{S}_i(z+1). \quad (42)$$

289 We can compute its spectral weight

$$S_\varphi(\omega, q_z, \mathbf{q}) = -2\text{Im} G_\varphi^{q_z}(q) \Big|_{i\omega \rightarrow \omega + i0^+}, \quad (43)$$

290 where  $G_\varphi^{q_z}(q)$  is the Fourier transform of Eq.(39). The result is

$$S_\varphi(\omega, q_z, \mathbf{q}) \sim \frac{1}{N_b} \Theta(|\omega| - |\mathbf{q}|) \text{sign}(\omega) (\omega^2 - |\mathbf{q}|^2)^{\frac{1}{2} + \Delta_{q_z}^{(1)}} \cos(\pi \Delta_{q_z}^{(1)}). \quad (44)$$

291 It shows ‘local criticality’ along  $z$ -direction, in the sense that  $S(\omega, q_z, \mathbf{q} = 0)$  has zero energy  
292 excitation in the whole range of  $q_z \in [0, 2\pi)$ . This means that we cannot do scaling and RG  
293 flow of  $q_z$  direction at all.

294 By Fourier transforming Eq. 39, we can learn about how the correlation function of  $\varphi_z$   
295 decays in  $z$ -direction. Notice that Eq. 39 is only valid in a large distance of  $x$ , and we have  
296 little knowledge about the UV physics at  $x = 0$  limit. Our strategy is to fix a large but finite  
297  $x$ , and then see how the correlation function  $G_\varphi^{z-z'}(x)$  vary as we increase  $z - z'$ . Notice that  
298 in Eq. 39, the  $q_z$  dependence is reflected in the power of  $1/x^2 \Lambda^2$ . So we cannot obtain the  
299 asymptotic form  $G_\varphi^{z-z'}(x) \sim g_\varphi(z-z') \frac{1}{|x|^{d_\varphi}}$ , since the dependence on  $z$  and  $x$  are not separated.  
300 What we can do is the following integral

$$g(z-z'; x\Lambda) = \frac{1}{2\pi} \int_0^{2\pi} dq_z e^{iq_z \cdot (z-z')} \left( \frac{1}{x^2 \Lambda^2} \right)^{\Delta_{q_z}^{(1)}} \quad (45)$$

301 at a fixed  $1/x^2 \Lambda^2$ . The numerical result is in Fig. 5. We can see that at a fixed  $x$ , the correlation  
302 function  $G_\varphi^{z-z'}$  exponentially decay in  $z$  direction. However, the correlation length also depends  
303 on  $x$ .  $G_\varphi^{z-z'}(x)$  now is

$$G_\varphi^{z-z'}(x) = g(z-z'; x\Lambda) \left( \frac{8}{\pi^2 N_b |x|^4} \right). \quad (46)$$

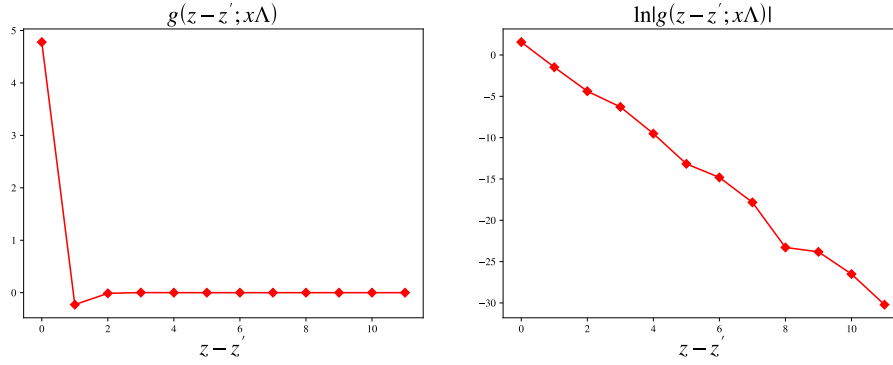


Figure 5: The numerical result of  $g(z-z'; x\Lambda)$  in Eq. 45, which characterizes the decay of the correlation function of  $|\Phi|^2$  in  $z$ -direction for a fixed  $x$ . We have chosen the parameters  $N_b = 2$ ,  $\alpha = 2$  and  $(1/x^2\Lambda^2) = 0.05$ . The logarithm of  $g(z-z'; x\Lambda)$  is also plotted which shows the exponential decay.

304 Correlation functions of other physical operators can also be studied. We list the physical  
 305 quantities and their expressions at both the critical point and the 3D phase in Table. 1. For  
 306 example, consider the correlation function of  $b_3 = \partial_1 a_2 - \partial_2 a_1$ . Using the effective propagator  
 307 Eq. 38, we can see that the leading order is already  $q_z$  dependent and is as follows:

$$\langle b_3^{q_z}(q) b_3^{-q_z}(q) \rangle = \left( \frac{1}{N_b} \cdot \frac{\pi^2 \sin^2(\frac{q_z}{2})}{\alpha^2 + \frac{1}{4}\pi^2 \sin^4(\frac{q_z}{2})} \right) \frac{q_1^2 + q_2^2}{|q|}. \quad (47)$$

308 For the correlation function of  $b_3$ , the  $q_z$  dependence is in a prefactor separated from the  $q$   
 309 dependence. So when we Fourier transform it to real space, the Fourier transformations into  
 310  $z$  and into  $x$  are independent of each other:

$$\langle b_3^z(x) b_3^{z'}(0) \rangle = g_{b_3}(z-z') \mathcal{F}_{b_3}(x), \quad (48)$$

$$g_{b_3}(z-z') = \frac{1}{2\pi} \int_0^{2\pi} dq_z e^{iq_z(z-z')} \frac{1}{N_b} \cdot \frac{\pi^2 \sin^2(\frac{q_z}{2})}{\alpha^2 + \frac{1}{4}\pi^2 \sin^4(\frac{q_z}{2})}, \quad (49)$$

311 where  $\mathcal{F}_{b_3}(x) \sim 1/x^4$  by dimensional analysis. The numerical result of  $g_{b_3}(z-z')$  is in Fig. 6.  
 312 We can see that the correlation function  $b_3$  exponentially decays in  $z$ -direction. This time, the  
 313 correlation length in  $z$ -direction is independent of  $x$ .

## 314 5 Continuous transition between gapped fracton order and gap- 315 less 3D phase

316 Our 2D to 3D transition of CSL can be easily generalized to the fractional quantum Hall phase.  
 317 For example, the same theory (with a different level of the Chern-Simons term) can describe  
 318 a transition between decoupled  $1/3$  Laughlin state and a gapless 3D quantum Hall phase  
 319 proposed in Ref. [28]. In this section, we try to make a more non-trivial generalization.

### 320 5.1 2D iCSM theory

321 The decoupled CSL or Laughlin state is described by a  $K$  matrix with dimension  $N \times N$ , where  
 322  $N$  as usual is the number of layers. For the decoupled CSL or Laughlin state, the  $K$  matrix only

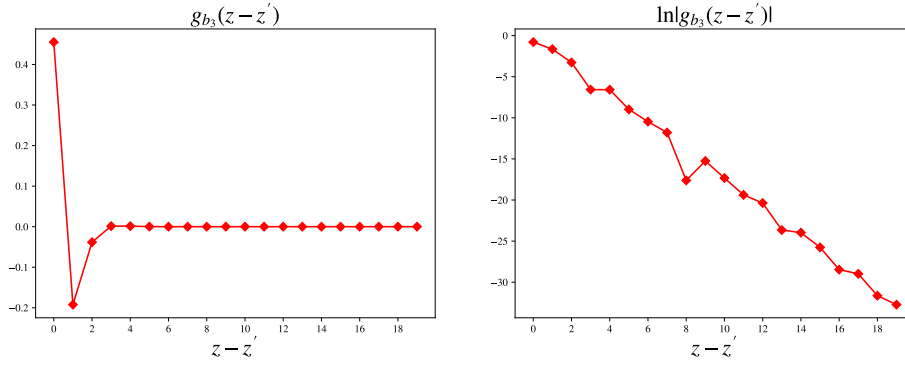


Figure 6: The numerical result of  $g_{b_3}(z-z')$  in Eq. 49, which characterizes the decay of the correlation function of  $b_3$  in  $z$ -direction. We have chosen the parameters  $N_b = 2$ ,  $\alpha = 2$ . The logarithm of  $g_{b_3}(z-z')$  is also plotted which shows the exponential decay.

323 has diagonal elements. But one can easily imagine a phase with also off-diagonal elements in  
 324 the  $N \times N$   $K$  matrix. A more general  $K$  matrix was discussed previously [29–31] and called  
 325 infinite component Chern-Simons-Maxwell(iCSM) theory. The effective action is

$$S_{2D,iCSM} = \frac{i}{4\pi} \sum_{z,z'} K_{z,z'} \int d^3x \epsilon_{\mu\nu\rho} a_\mu^z \partial_\nu a_\rho^{z'} + \frac{1}{4g^2} \sum_z \int d^3x (\partial_\mu a_\nu^z - \partial_\nu a_\mu^z)^2. \quad (50)$$

326 For simplicity, let us consider a  $K$  matrix in the form:

$$K_{z,z'} = \begin{pmatrix} c_0 & c_1 & & & c_1 \\ c_1 & c_0 & c_1 & & \\ & \ddots & \ddots & \ddots & \\ & & c_1 & c_0 & c_1 \\ c_1 & & & c_1 & c_0 \end{pmatrix}, \quad (51)$$

327 which has translational symmetry along the  $z$  direction so we can employ a Fourier trans-  
 328 formation to diagonalize it. This theory describes a phase with dispersion relation

$$\omega^2 = \mathbf{q}^2 + C(q_z)^2 g^4, \quad (52)$$

329 where  $C(q_z) = \frac{1}{2\pi} (c_0 + 2c_1 \cos q_z)$ ,  $q_z = 0, \frac{2\pi}{N}, \dots, \frac{2\pi}{N}(N-1)$  is the Fourier momentum in  $z$   
 330 direction. To avoid complexity, we take the limit  $N \rightarrow \infty$  so  $q_z$  can be any rational or irrational  
 331 number  $\in [0, 2\pi)$ . We can see that when the ratio  $|c_0/2c_1| > 1$ ,  $C(q_z)$  is always nonzero and  
 332 the energy dispersion Eq. 52 has a minimum energy

$$\omega_{\min} = \frac{g^2}{2\pi} (|c_0| - 2|c_1|) \quad (53)$$

333 which occurs at either  $q_z = 0$  or  $q_z = \pi$  depending on the relative sign of  $c_0$  and  $c_1$ . In this  
 334 case, the photon has a large gap. However, with other values of the ratio  $c_0/2c_1$ , the photon  
 335 can also be gapless in the 2D iCSM.

336 When the ratio  $|c_0/2c_1| = 1$ ,  $C(q_z) = 0$  at  $q_z^*$  which equals to 0 or  $\pi$ . The photon is gapless  
 337 with a quadratic dispersion in  $q_z$ :

$$\omega^2 = \mathbf{q}^2 + \frac{c_0^2 g^4}{16\pi^2} (q_z - q_z^*)^4, \quad |q_z - q_z^*| \ll 1. \quad (54)$$



338 When the ratio  $|c_0/2c_1| < 1$ ,  $C(q_z) = 0$  at  $q_z^* = \pm \arccos(-c_0/2c_1)$ . The photon is gapless  
339 with a linear dispersion in  $q_z$ :

$$\omega^2 = \mathbf{q}^2 + \frac{(4c_1^2 - c_0^2)g^4}{4\pi^2} (q_z^2 - q_z^*)^2, \quad |q_z - q_z^*| \ll 1. \quad (55)$$

340 Other interesting features of this 2D iCSM are discussed in Ref. [29]. For example, when  
341  $c_0/2c_1 > 1$ , we can get the inverse of the  $K$  matrix when  $N \rightarrow \infty$ :

$$(K^{-1})_{z,z'} \rightarrow \frac{(-1)^{z-z'}}{2c_1 \sqrt{\left(\frac{c_0}{2c_1}\right)^2 - 1}} \left( \frac{c_0}{2c_1} + \sqrt{\left(\frac{c_0}{2c_1}\right)^2 - 1} \right)^{-|z-z'|}. \quad (56)$$

342 In Ref. [29], the author chose  $c_0 = 3, c_1 = 1$ . This describes a gapped phase with quite  
343 strange statistics  $\theta_{z,z'} = 2\pi \frac{(-1)^{z-z'}}{\sqrt{5}} \left(\frac{3+\sqrt{5}}{2}\right)^{-|z-z'|}$ , which decay exponentially when  $z-z'$  grows,  
344 but never become exactly zero. It was called non-foliated fracton order [29].

## 345 5.2 3D iCSM theory: a gapless phase

346 The U(1) gauge field in the iCSM theory is still 2+1d. Now we consider a phase transition after  
347 which it becomes 3+1d. As before we simply consider the onset of a term  $\sum_z \Phi(z) b^\dagger(z) b(z+1)$   
348 where  $b(z)$  is the operator carrying charge 1 under the gauge field in the  $z$  layer. Then this  
349 term makes the U(1) gauge field 3D, similar to our previous discussions on the 3D CSL phase.  
350 Let us first understand its property. The action now is:

$$S_{3D,iCSM} = \frac{i}{4\pi} \sum_{z,z'} K_{z,z'} \int d^3x \epsilon_{\mu\nu\rho} a_\mu^z \partial_\nu a_\rho^{z'} + \frac{1}{4g^2} \sum_z \int d^3x (\partial_\mu a_\nu^z - \partial_\nu a_\mu^z)^2 \\ + \frac{\rho_s}{2} \sum_z \int d^3x (\partial_\mu a_z - (a_\mu^{z+1} - a_\mu^z))^2. \quad (57)$$

351 Note that we can use the gauge  $a_z = 0$ , so the  $\rho_s$  term just looks like a Higgs term (see  
352 Eq. 25):

$$S_{\text{int}} = \frac{1}{2} \sum_{q_z} \int \frac{d^3q}{(2\pi)^3} u(q_z) a_\mu^{q_z}(q) \left( \delta_{\mu\nu} - \frac{q_\mu q_\nu}{q^2} \right) a_\nu^{-q_z}(-q), \quad (58)$$

353 where  $\mu, \nu = 0, 1, 2$ ,  $q_z = 0, \frac{2\pi}{N}, \dots, \frac{2\pi(N-1)}{N}$  is the discrete momentum in  $z$ -direction, the coeffi-  
354 cient  $u(q_z) = 4\rho_s \sin^2(q_z/2)$ .

355 In our discussion, we assume that the matrix  $K_{z,z'}$  only includes diagonal and the nearest  
356 neighbor terms,  $K_{z,z'} = c_0 \delta_{z,z'} + c_1 \delta_{z,z'+1} + c_1 \delta_{z,z'-1}$ . Fourier transforming the action Eq.(57),  
357 we get:

$$S_{3D,iCSM} = \frac{1}{2} \sum_{q_z} \int \frac{d^3q}{(2\pi)^3} a_\mu^{q_z}(q) \left( C(q_z) \epsilon_{\mu\rho\nu} q_\rho + \left( \frac{1}{g^2} q^2 + u(q_z) \right) \left( \delta_{\mu\nu} - \frac{q_\mu q_\nu}{q^2} \right) \right) a_\nu^{-q_z}(-q), \quad (59)$$

358 where  $C(q_z) = \frac{1}{2\pi} (c_0 + 2c_1 \cos q_z)$ ,  $u(q_z) = 4\rho_s \sin^2 \frac{q_z}{2}$ . By doing the matrix inverse in the  
359 transverse subspace, we obtain the photon propagator

$$D_{\mu\nu}^{q_z}(q) = \frac{-C}{C^2 q^2 + \left(\frac{q^2}{g^2} + u(q_z)\right)^2} \epsilon_{\mu\nu\rho} q_\rho + \frac{\frac{q^2}{g^2} + u(q_z)}{C^2 q^2 + \left(\frac{q^2}{g^2} + u(q_z)\right)^2} \left( \delta_{\mu\nu} - \frac{q_\mu q_\nu}{q^2} \right). \quad (60)$$

360 From its poles, we can obtain the dispersion relations. We get two modes with dispersion  
361 relations

$$\omega_{\pm}^2 = \mathbf{q}^2 + \frac{1}{2} \left( C(q_z)^2 g^4 + 2u(q_z)g^2 \pm \sqrt{C(q_z)^4 g^8 + 4C(q_z)^2 u(q_z)g^6} \right). \quad (61)$$

362 The reason why we get two photon modes here instead of one mode in 2D iCSM is the  
363 same as in Sec. 3: after the condensation transition, the phase of the condensate serve as a  
364 new gauge field component, so the gauge field is now 3+1 d. We know that there can be two  
365 polarizations in 3+1 d  $U(1)$  gauge theory. The difference of Eq. 61 from the energy dispersion  
366 in Sec. 3 is that there is a  $q_z$  dependent function  $C(q_z)$  which comes from the inter-layer mutual  
367 coupling  $K_{z,z'}$ . The low energy dispersion relations are summarized in Fig. 7. We can see that  
368 in 3D iCSM, the new photon mode  $\omega_-$  is always gapless for all values of  $c_0/2c_1$ . For most  
369 situations,  $\omega_-$  is quadratic in small  $q_z$  while when  $c_0/2c_1 = -1$  it is linear in small  $q_z$ .

370 We also discussed the electromagnetic response of the 3D iCSM theory in Appendix. D.  
371 Both  $\sigma_{xx}$  and  $\sigma_{xy}$  vanish in the DC ( $\omega = 0$ ) limit at finite  $q_z \neq 0$ , like a trivial insulator. Only  
372 at  $q_z = 0$ ,  $\sigma_{xx}^{q_z=0}(\omega = 0) = 0$  and  $\sigma_{xy}^{q_z=0}(\omega = 0) = \frac{1}{c_0+2c_1} \frac{e^2}{h}$ , like a FQHE insulator.

### 373 5.3 Critical theory between gapped fracton order and gapless 3D phase

374 Similar to Eq. 30, we can also write down the critical theory at the transition point  $g = g_c(c_0, c_1)$   
375 and the only difference from Eq. 30 is the Chern-simons term:

$$S = \sum_z \int d^3x |(\partial_\mu - i(a_\mu^{z+1} - a_\mu^z))\Phi_z|^2 + \frac{i}{4\pi} \sum_{z,z'} K_{z,z'} \int d^3x \epsilon_{\mu\nu\rho} a_\mu^z \partial_\nu a_\rho^{z'} \\ + \frac{1}{2} \sum_{z,z'} \lambda_{z,z'} \int d^3x |\Phi_z|^2 |\Phi_{z'}|^2, \quad (62)$$

376 where  $\Phi_z$  is the condensate field between layer  $z$  and  $z+1$ . We can still use the large  $N_b$   
377 expansion we used in Sec. 4 to study the critical behavior. The only difference is in the bare  
378 photon propagator. Note that  $|c_0/2c_1| > 1$  is required for the  $K$  matrix to be inverted. For  
379 example, when  $c_0 = 3$ ,  $c_1 = 1$ , We can get the bare photon propagator:

$$D_{0,\mu\nu}^{q_z}(q) = -\frac{2\pi}{N_b} \frac{\epsilon_{\mu\lambda\nu} q_\lambda}{q^2} \frac{1}{3 + 2\cos q_z}, \quad (63)$$

380 or in real space:

$$D_{0,\mu\nu}^{z,z'}(q) = -\frac{2\pi}{N_b} \frac{\epsilon_{\mu\lambda\nu} q_\lambda}{q^2} (K)_{z,z'}^{-1}, \quad (64)$$

381 where from Eq. 56 we have

$$(K)_{z,z'}^{-1} = \frac{(-1)^{z-z'}}{\sqrt{5}} \left( \frac{3 + \sqrt{5}}{2} \right)^{-|z-z'|}. \quad (65)$$

382 Unlike Eq. 32, where the bare photon propagator is diagonal in  $z, z'$ , here the bare photon  
383 propagator already has off-diagonal terms. In other words, the bare photon propagator is  
384 already  $q_z$  dependent in momentum space. We can further calculate the large  $N_b$  effective  
385 photon propagator

$$D_{\text{eff},\mu\nu}^{q_z}(q) = \frac{2\pi/(3 + 2\cos q_z)}{1 + \frac{\pi^2 \sin^4 \frac{q_z}{2}}{4(3 + 2\cos q_z)^2}} \left( \frac{\pi \sin^2 \frac{q_z}{2}}{2(3 + 2\cos q_z)|q|} \left( \delta_{\mu\nu} - \frac{q_\mu q_\nu}{q^2} \right) - \frac{\epsilon_{\mu\nu\lambda} q_\lambda}{q^2} \right) + \mathcal{O}(1/N_b^2), \quad (66)$$

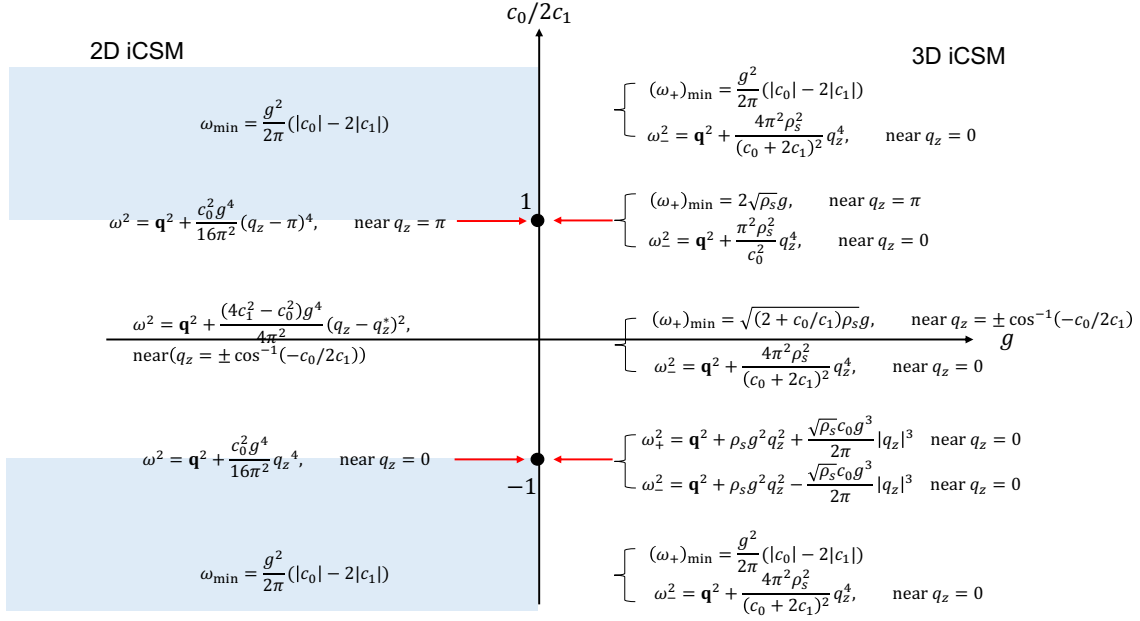


Figure 7: Phase diagram of the iCSM theory.  $g$  is the control parameter driving the system go through the transition from 2D iCSM to 3D iCSM. The shaded regions represent the gapped phase while others are the gapless phase. The dispersion relations are not valid near the critical region  $g = g_c$ , whose properties need more careful studies.

386 which is also  $q_z$  dependent, and see that the photon energy is still zero for any  $q_z$  as long as  
 387  $\mathbf{q} = 0$ . This slight difference in the bare photon propagator will not change the overall critical  
 388 behavior we discussed in Sec. 4.

## 389 6 Conclusion

390 In summary, we propose a general framework to understand the 2D to 3D transition of a frac-  
 391 tional phase with a U(1) gauge field in a system with infinitely stacked 2D layers. We applied it  
 392 to the case of chiral spin liquid (or fractional quantum Hall phase). The 3D phase of the chiral  
 393 spin liquid (CSL) has a gapless photon mode. The 2D to 3D transition is described by the Higgs  
 394 transition of a boson  $\Phi$ , which becomes critical at each layer. Interestingly, we find that the  
 395 critical mode is gapless along a line  $(q_x, q_y, q_z) = (0, 0, q_z)$  for any  $q_z \in [0, 2\pi)$ , but the scaling  
 396 dimension has a  $q_z$  dependence. As a result, gauge invariant operators have a finite but non-  
 397 zero correlation length in the  $z$ -direction. Besides, our theory can be generalized to describe a  
 398 continuous phase transition between a fracton phase described by infinite component Chern  
 399 Simons theory and a 3D gapless phase similar to the 3D CSL. In the future, we hope to make  
 400 the matter field also gapless at the critical point. For example, we can generalize the current  
 401 framework to describe the 2D to 3D transition of composite Fermi liquid, Dirac spin liquid,  
 402 and spinon Fermi surface phases. It is also interesting to study metal-insulator transition in  
 403 quasi 2D system [39] with 2D or 3D spin liquid in the insulator side.

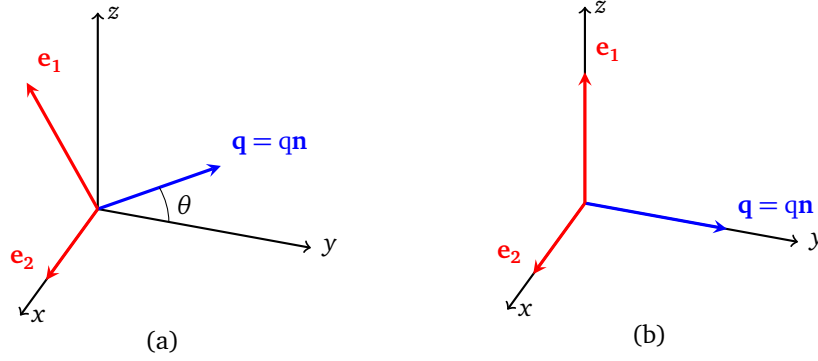


Figure 8: Definition of vectors we use to calculate the photon polarizations. Unit vectors  $\mathbf{e}_1$ ,  $\mathbf{e}_2$  and  $\mathbf{n}$  form a right-hand orthonormal system.  $\mathbf{n}$  lies in the  $y$ - $z$  plane and represents the direction of wave vector  $\mathbf{q}$ .  $\mathbf{e}_2$  is always pointing in the  $x$ -direction. (a) is for nonzero  $\theta$  case and (b) is for  $\theta = 0$  case.

## 404 Acknowledgements

405 YHZ thanks Ashvin Vishwanath for discussions at initial stage of the work. This work was  
 406 supported by the National Science Foundation under Grant No. DMR2237031. This work  
 407 was performed in part at Aspen Center for Physics, which is supported by National Science  
 408 Foundation grant PHY-2210452.

## 409 A Plane-wave solution to the Maxwell equations

410 The new set of “Maxwell’s equations” in the 3D CSL phase is as follows:

$$\nabla \cdot \vec{e} + (\tilde{\rho}_s g^2 - 1) \partial_z e_z - \frac{k g^2}{2\pi} b_z = 0, \quad (\text{A.1})$$

$$\partial_t \vec{e} - \nabla \times \vec{b} - (\tilde{\rho}_s g^2 - 1) \partial_z (\hat{z} \times \vec{b}) - \frac{k g^2}{2\pi} \hat{z} \times \vec{e} = 0, \quad (\text{A.2})$$

$$\nabla \cdot \vec{b} = 0, \quad (\text{A.3})$$

$$\nabla \times \vec{e} + \partial_t \vec{b} = 0. \quad (\text{A.4})$$

411 To find the plane-wave solution  $\vec{e} = \mathcal{E} e^{i\mathbf{q}\cdot\mathbf{x} - i\omega t}$ ,  $\vec{b} = \mathcal{B} e^{i\mathbf{q}\cdot\mathbf{x} - i\omega t}$  to the equations above, we  
 412 set  $\mathbf{q}$  lying in the  $y$ - $z$  plane due to the rotational symmetry about the  $z$ -axis. Eq. A.3 is then  
 413  $\mathbf{n} \cdot \mathcal{B} = 0$ , so  $\mathcal{B} = B_1 \mathbf{e}_1 + B_2 \mathbf{e}_2$  where  $\mathbf{e}_1 = (0, -\sin \theta, \cos \theta)$ ,  $\mathbf{e}_2 = (1, 0, 0)$ . Using Eq. A.1 and  
 414 Eq. A.4, we get  $\mathcal{E} = \frac{\omega B_2}{q} \mathbf{e}_1 - \frac{\omega B_1}{q} \mathbf{e}_2 + \frac{\omega B_2 \sin \theta \cos \theta (1 - \tilde{\rho}_s g^2) - \frac{i k g^2}{2\pi} B_1 \cos \theta}{q(\cos^2 \theta + \tilde{\rho}_s g^2 \sin^2 \theta)} \mathbf{n}$ . Plug them into Eq. A.2,  
 415 we get

$$\begin{pmatrix} \frac{k g^2 \omega \sin \theta}{2\pi} & -i(\omega^2 - q^2) + i(\tilde{\rho}_s g^2 - 1)q_z^2 \\ i(\omega^2 - q^2) - i(\tilde{\rho}_s g^2 - 1)q_z^2 - \frac{i k^2 g^4 \cos^2 \theta}{4\pi^2(\cos^2 \theta + \tilde{\rho}_s g^2 \sin^2 \theta)} & -\frac{k \tilde{\rho}_s g^4 \omega \sin \theta}{2\pi(\cos^2 \theta + \tilde{\rho}_s g^2 \sin^2 \theta)} \end{pmatrix} \begin{pmatrix} B_1 \\ B_2 \end{pmatrix} = 0. \quad (\text{A.5})$$

416 For plane wave solutions to exist, the determinant of the large matrix should vanish. Solv-  
 417 ing this equation gives us two dispersion relations  $\omega_{\pm}$  and the corresponding two eigenmodes  
 418  $\mathcal{B}_{\pm}$ :

$$\omega_{\pm}^2 = q_x^2 + q_y^2 + \tilde{\rho}_s g^2 q_z^2 + \frac{k^2 g^4}{8\pi^2} \pm \frac{k^2 g^4}{8\pi^2} \sqrt{1 + \frac{16\pi^2 \tilde{\rho}_s}{k^2 g^2} q_z^2} \quad (\text{A.6})$$

$$\mathcal{B}_+ = \mathbf{e}_1 + \frac{ik \left( -\cos^2 \theta + \tilde{\rho}_s g^2 \sin^2 \theta + (\cos^2 \theta + \tilde{\rho}_s g^2 \sin^2 \theta) \sqrt{1 + \frac{16\pi^2 \tilde{\rho}_s}{k^2 g^2} q_z^2} \right)}{\sqrt{2} \tilde{\rho}_s \sin \theta \sqrt{8\pi^2 q^2 (\cos^2 \theta + \tilde{\rho}_s g^2 \sin^2 \theta) + k^2 g^4 + k^2 g^4 \sqrt{1 + \frac{16\pi^2 \tilde{\rho}_s}{k^2 g^2} q_z^2}}} \mathbf{e}_2, \quad (\text{A.7})$$

$$\mathcal{B}_- = \frac{i\sqrt{2} \tilde{\rho}_s \sin \theta \sqrt{8\pi^2 q^2 (\cos^2 \theta + \tilde{\rho}_s g^2 \sin^2 \theta) + k^2 g^4 - k^2 g^4 \sqrt{1 + \frac{16\pi^2 \tilde{\rho}_s}{k^2 g^2} q_z^2}}}{k \left( \cos^2 \theta - \tilde{\rho}_s g^2 \sin^2 \theta + (\cos^2 \theta + \tilde{\rho}_s g^2 \sin^2 \theta) \sqrt{1 + \frac{16\pi^2 \tilde{\rho}_s}{k^2 g^2} q_z^2} \right)} \mathbf{e}_1 + \mathbf{e}_2. \quad (\text{A.8})$$

419 We can look at the special case where  $\theta = 0$  (see Fig. 8). Here  $\mathcal{B}_{\pm}$  both become linearly  
 420 polarized:  $\mathcal{B}_+ = \mathbf{e}_1$  and  $\mathcal{B}_- = \mathbf{e}_2$ . Remember that in 2+1 d Chern-Simons theory, there is only  
 421 one gapped mode and the magnetic field only has a z-component. Here  $\mathcal{B}_+$  looks very similar  
 422 to that mode: it is linearly polarized in the z-direction and has a large energy gap which goes  
 423 to infinity as  $g^2 \rightarrow \infty$  as in 2 + 1 d Chern-Simons theory. The other gapless mode  $\mathcal{B}_-$  lies  
 424 in the x-y plane, which cannot exist unless we have the fourth component of the gauge field.  
 425 So starting from the 2D CSL, the gapped photon mode remains gapped across the transition,  
 426 while a new gapless mode emerges after the transition.

## 427 B Effective propagators

428 We consider the effective photon propagator first. In the large  $N_b$  limit, all the bubble diagrams  
 429 (see Fig. 3) are of order unity so we should add them together (a boson loop has factor  $N_b$  and a  
 430 bare propagator has factor  $1/N_b$ ). Given the definition  $\langle \alpha_{\mu}^z(q) \alpha_{\nu}^{z'}(-q) \rangle = (2\pi)^3 \delta^3(q-q') \tilde{D}_{\mu\nu}^{z-z'}(q)$ ,  
 431 we have a Dyson equation

$$\tilde{D}_0(q) + \tilde{D}_0(q) \tilde{\Pi}(q) \tilde{D}_{\text{eff}}(q) = \tilde{D}_{\text{eff}}(q), \quad (\text{B.1})$$

432 where the layer and space-time indices are ignored. The self-energy is

$$\tilde{\Pi}_{\mu\nu}^{z,z'}(q) = N_b \delta^{z,z'} \int \frac{d^3 p}{(2\pi)^3} \frac{(2p+q)_{\mu} (2p+q)_{\nu}}{(q+p)^2 p^2} = -\frac{N_b}{16} \delta^{z,z'} |q| \left( \delta_{\mu\nu} - \frac{q_{\mu} q_{\nu}}{q^2} \right). \quad (\text{B.2})$$

433 The solution to this equation is  $\tilde{D}_{\text{eff}}(q) = (\mathbf{1}(q) - \tilde{D}_0(q) \tilde{\Pi}(q))^{-1} \tilde{D}_0(q)$ , where  $\mathbf{1}(q) = \delta^{z,z'} \left( \delta_{\mu\nu} - \frac{q_{\mu} q_{\nu}}{q^2} \right)$   
 434 is the projection operator into transverse subspace since we work in Landau gauge. The matrix  
 435 inverse is also done in the transverse subspace. It is convenient to go to  $q_z$  space and the result  
 436 is

$$\tilde{D}_{\text{eff},\mu\nu}^{q_z}(q) = \frac{A(q_z)}{N_b} \left( \frac{B(q_z)}{|q|} \left( \delta_{\mu\nu} - \frac{q_{\mu} q_{\nu}}{q^2} \right) - \frac{\epsilon_{\mu\nu\lambda} q_{\lambda}}{q^2} \right) + \mathcal{O}(1/N_b^2), \quad (\text{B.3})$$

437 where we introduced

$$A(q_z) = \frac{8\pi}{\alpha} \frac{\sin^2 \frac{q_z}{2}}{1 + \frac{\pi^2 \sin^4 \frac{q_z}{2}}{4\alpha^2}}, \quad B(q_z) = \frac{\pi \sin^2 \frac{q_z}{2}}{2\alpha}. \quad (\text{B.4})$$

438 In real x space it is

	$= \langle \alpha_\mu^i(x) \alpha_\nu^j(0) \rangle_{\text{eff}}$
	$= \frac{1}{4\pi x } \delta_{ij}$
	$= -\delta_{\mu\nu}$
	$= i \overleftrightarrow{\partial}_\mu^x$
	$= \langle \varphi_i(x) \varphi_j(0) \rangle_{\text{eff}}$
	$= -1$

Table 3: Feynman rules. All propagators are diagonal in the flavor index; All vertices conserve the flavor index.

$$\tilde{D}_{\text{eff},\mu\nu}^{q_z}(x) = \frac{A(q_z)}{4\pi^2 N_b} \left( \frac{4B(q_z)x_\mu x_\nu}{|x|^4} + \frac{i\pi\epsilon_{\mu\nu\lambda} x_\lambda}{|x|^3} \right). \quad (\text{B.5})$$

439 The effective propagator  $G_{\varphi,\text{eff}}$  is also given by bubble diagram summation. Given the  
 440 definition  $\langle \varphi_z(p) \varphi_{z'}(-p') \rangle = (2\pi)^3 \delta^3(p-p') G_\varphi^{ij}(p)$ , we have a Dyson equation

$$G_{\varphi,0}(p) + G_{\varphi,0}(p) \Pi_\varphi(p) G_{\varphi,\text{eff}}(p) = G_{\varphi,\text{eff}}(p), \quad (\text{B.6})$$

441 where  $G_{\varphi,0}^{z,z'} = -\lambda_{z,z'}$ . The self-energy  $\Pi_\varphi^{z,z'}(p) = -N_b \delta^{z,z'} \int \frac{d^3q}{(2\pi)^3} \frac{1}{(q+p)^2 q^2} = -N_b \frac{\delta^{z,z'}}{8|p|}$ . The  
 442 solution to this equation is  $G_{\varphi,\text{eff}}(p) = (1 - G_{\varphi,0}(p) \Pi_\varphi(p))^{-1} G_{\varphi,0}(p)$ . The result is

$$G_{\varphi,\text{eff}}^{q_z} = -\frac{8|p|}{N_b} + \mathcal{O}(1/N_b^2). \quad (\text{B.7})$$

443 In real  $x$  and  $z$  space, it is

$$G_{\varphi,\text{eff}}^{z-z'}(x) = \frac{8}{\pi^2 N_b |x|^4} \delta^{z,z'}. \quad (\text{B.8})$$

## 444 C Feynman diagram calculation

445 All the diagrams and their results are in Table. 2, and the Feynman rules are in Table. 3. We  
 446 also show the calculation of several typical diagrams in Table. 2. Notice that the result of  
 447 an individual diagram might depend on the gauge choosing, but the sum of them should not  
 448 since  $\varphi$  is a gauge-independent operator. We use a UV cutoff  $\Lambda$  to regularize the divergent  
 449 momentum integrals. We only keep the logarithmic divergence, so for every  $n \neq 3$ ,  $\int \frac{d^3q}{q^n}$  is  
 450 regarded as 0. To avoid confusion with the integral variable, we use  $i, j$  as the layer index in  
 451 this section.

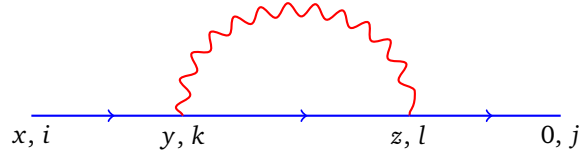


Figure 9: Subdiagram B': loop correction to the boson propagator

452 First, we consider Graph B. Comparing to Graph A, there is a boson loop giving factor  $N_b$ ,  
 453 a photon propagator giving factor  $1/N_b$  and an extra  $G_{\varphi,\text{eff}}$  giving factor  $1/N_b$  so the overall  
 454 order is of  $1/N_b$ . The two  $G_{\varphi,\text{eff}}$ 's near the ends don't contribute to logarithmic divergence  
 455 since in momentum representation, they are just multiplying factors  $1/p^2$ . Therefore we only  
 456 need to calculate the logarithmic divergence in the region surrounded by the boson loop (this  
 457 applies to all the diagrams in Table. 2). It turns out we can calculate the subdiagram B' in  
 458 Fig. 9.

$$\begin{aligned}
 \text{Graph B}' &= \sum_k \sum_l \int d^3y d^3z \left( \frac{\delta_{ik}}{4\pi|x-y|} \right) i \overleftrightarrow{\partial}_\mu^y \left( \frac{\delta_{kl}}{4\pi|y-z|} \right) i \overleftrightarrow{\partial}_\nu^z \left( \frac{\delta_{lj}}{4\pi|z|} \right) \cdot \tilde{D}_{\text{eff},\mu\nu}^{kl}(y-z) \\
 &= \delta_{ij} \int d^3y d^3z \left( \frac{1}{4\pi|x-y|} \right) i \overleftrightarrow{\partial}_\mu^y \left( \frac{1}{4\pi|y-z|} \right) i \overleftrightarrow{\partial}_\nu^z \left( \frac{1}{4\pi|z|} \right) \cdot \frac{1}{N} \sum_{q_z} \tilde{D}_{\text{eff},\mu\nu}^{q_z}(y-z) \\
 &= \delta_{ij} \int \frac{d^3p}{(2\pi)^3} \frac{e^{ip \cdot x}}{p^4} \left[ \frac{1}{N} \sum_{q_z} \int \frac{d^3q}{(2\pi)^3} \frac{(2p+q)_\mu (2p+q)_\nu}{(q+p)^2} \tilde{D}_{\text{eff},\mu\nu}^{q_z}(-q) \right] \\
 &= \delta_{ij} \int \frac{d^3p}{(2\pi)^3} \frac{e^{ip \cdot x}}{p^4} \left[ \frac{1}{N} \sum_{q_z} \int \frac{d^3q}{(2\pi)^3} \frac{(2p+q)_\mu (2p+q)_\nu}{(q+p)^2} \right. \\
 &\quad \left. \times \frac{A(q_z)}{N_b} \left( \frac{B(q_z)}{|q|} (\delta_{\mu\nu} - \frac{q_\mu q_\nu}{q^2}) - \frac{\epsilon_{\mu\nu\lambda} q_\lambda}{q^2} \right) \right].
 \end{aligned} \tag{C.1}$$

459 We do the  $q$  integral first. Using  $\frac{1}{(p+q)^2} = \frac{1}{q^2} - \frac{2q \cdot p + p^2}{q^4} + \frac{4(p \cdot q)^2}{q^6} + \mathcal{O}(\frac{1}{q^6})$ , we obtain its logarithmic  
 460 divergence to be

$$\begin{aligned}
 \text{Graph B}' &= \delta_{ij} \int \frac{d^3p}{(2\pi)^3} \frac{e^{ip \cdot x}}{p^4} \left[ \frac{1}{N_b N} \sum_{q_z} A(q_z) B(q_z) \int \frac{d^3q}{(2\pi)^3} \frac{4p_\mu p_\nu}{|q|^3} (\delta_{\mu\nu} - \frac{q_\mu q_\nu}{q^2}) \right] \\
 &= \delta_{ij} \int \frac{d^3p}{(2\pi)^3} \frac{e^{ip \cdot x}}{p^4} \left[ \frac{1}{N_b N} \sum_{q_z} A(q_z) B(q_z) \cdot 4p_\mu p_\nu \delta_{\mu\nu} (1 - \frac{1}{3}) \int \frac{d^3q}{(2\pi)^3} \frac{1}{|q|^3} \right],
 \end{aligned} \tag{C.2}$$

461 where we used  $\int d^d q f(q^2) q_\mu q_\nu = \frac{1}{d} \int d^d q q^2 f(q^2) \delta_{\mu\nu}$ . The last  $q$  integral is regularized by  
 462 cutoff momentum  $\Lambda$ :

$$\int \frac{d^3q}{(2\pi)^3} \frac{1}{|q|^3} = \frac{1}{4\pi^2} \ln x^2 \Lambda^2. \tag{C.3}$$

463 Here we use the dimensionless parameter  $x\Lambda$  inside the logarithmic function. So,

$$\begin{aligned}
 \text{Graph B}' &= \delta_{ij} \cdot \frac{2}{3\pi^2 N_b N} \sum_{q_z} A(q_z) B(q_z) \ln x^2 \Lambda^2 \cdot \int \frac{d^3p}{(2\pi)^3} \frac{e^{ip \cdot x}}{p^2} \\
 &= \delta_{ij} \cdot \frac{2}{3\pi^2 N} \sum_{q_z} A(q_z) B(q_z) \ln x^2 \Lambda^2 \cdot \left( \frac{1}{4\pi|x|} \right).
 \end{aligned} \tag{C.4}$$

464 Then using

$$\frac{1}{|x|^{2\alpha}} = \frac{\Gamma(\frac{d}{2} - \alpha)}{\pi^{\frac{d}{2}} 2^{2\alpha} \Gamma(\alpha)} \int d^d p \frac{e^{ip \cdot x}}{|p|^{d-2\alpha}}, \quad (\text{C.5})$$

465 we have

$$\int d^3 y d^3 z \left( \frac{8}{\pi^2 N_b |x-y|^4} \right) \left( \frac{1}{4\pi |y-z|} \right)^2 \left( \frac{8}{\pi^2 N_b |z|^4} \right) = -\frac{8}{\pi^2 N_b |x|^4}, \quad (\text{C.6})$$

466 so we get the result of Graph B in Table. 2.

467 Next, we consider the Graph F. In Graph F, there are two boson loops that contribute a factor  
468  $N_b^2$ , two photon propagators that contribute a factor  $1/N_b^2$ , and an extra  $G_{\varphi, \text{eff}}$  that contribute  
469 a factor  $1/N_b$ . So this diagram is of order  $1/N_b$  compared to Graph A. Again we calculate the  
470 amputated subdiagram without two external  $G_{\varphi, \text{eff}}$  first,

Graph F (amputated)

$$\begin{aligned} &= 4N_b^2 \int d^3 y d^3 z d^3 w \left( \frac{1}{4\pi |x-y|} \right)^2 (-\delta_{\mu\nu}) \tilde{D}_{\text{eff}, \mu\alpha}^{ij}(y-z) \tilde{D}_{\text{eff}, \nu\beta}^{ij}(y-w) \\ &\quad \times \left[ \frac{1}{4\pi |w|} i \overleftrightarrow{\partial}_\beta^w \frac{1}{4\pi |w-z|} i \overleftrightarrow{\partial}_\alpha^z \frac{1}{4\pi |z|} \right]. \end{aligned} \quad (\text{C.7})$$

471 Since  $\tilde{D}_{\text{eff}}(x) \propto 1/x^2$ , by power counting, the  $\ln \Lambda$  divergence might come from the region  
472 where  $y, z, w \rightarrow x$  or the region where  $y, z, w \rightarrow 0$ . In the first region, the logarithmic divergent  
473 part is

Region 1

$$\begin{aligned} &= -\frac{4N_b^2}{(4\pi |x|)^2} \int d^3 y d^3 z d^3 w \left( \frac{1}{4\pi |x-y|} \right)^2 \tilde{D}_{\text{eff}, \mu\alpha}^{ij}(y-z) \tilde{D}_{\text{eff}, \mu\beta}^{ij}(y-w) \cdot \left( \overrightarrow{\partial}_\beta^w \overrightarrow{\partial}_\alpha^z \frac{1}{4\pi |w-z|} \right) \\ &= -\frac{4N_b^2}{(4\pi |x|)^2} \int d^3 y' d^3 z' d^3 w' \left( \frac{1}{4\pi |y'|} \right)^2 \tilde{D}_{\text{eff}, \mu\alpha}^{ij}(-z') \tilde{D}_{\text{eff}, \mu\beta}^{ij}(-w') \cdot \left( \overrightarrow{\partial}_\beta^{w'} \overrightarrow{\partial}_\alpha^{z'} \frac{1}{4\pi |w'-z'|} \right) \end{aligned} \quad (\text{C.8})$$

474 where we introduced new integral variables  $y' = y - x$ ,  $z' = z - y$ ,  $w' = w - y$ . The  
475 integral over  $y'$  has no UV divergence ( $y' \rightarrow 0$ ); the remaining integral by power counting  
476 should be proportional to  $\int d^3 x/x^4$ , which is not a logarithmic divergence.

477 In the second region where  $y, z, w \rightarrow 0$ , the logarithmic divergent part is

Region 2

$$\begin{aligned} &= -\frac{4N_b^2}{(4\pi |x|)^2} \int d^3 y d^3 z d^3 w \tilde{D}_{\text{eff}, \mu\alpha}^{ij}(y-z) \tilde{D}_{\text{eff}, \mu\beta}^{ij}(y-w) \left[ \frac{1}{4\pi |w|} i \overleftrightarrow{\partial}_\beta^w \frac{1}{4\pi |w-z|} i \overleftrightarrow{\partial}_\alpha^z \frac{1}{4\pi |z|} \right] \\ &= -\frac{4N_b^2}{(4\pi |x|)^2} \frac{1}{N^2} \sum_{q_z, l_z} e^{iq_z \cdot (i-j)} \int \frac{d^3 p}{(2\pi)^3} \frac{d^3 q}{(2\pi)^3} \tilde{D}_{\text{eff}, \mu\alpha}^{l_z}(p) \tilde{D}_{\text{eff}, \mu\beta}^{q_z - l_z}(-p) \frac{(p+2q)_\alpha (p+2q)_\beta}{(p+q)^4 q^2} \\ &= -\frac{4}{(4\pi |x|)^2} \frac{1}{N^2} \sum_{q_z, l_z} e^{iq_z \cdot (i-j)} A(l_z) A(q_z - l_z) \int \frac{d^3 p}{(2\pi)^3} \frac{d^3 q}{(2\pi)^3} \frac{(p+2q)_\alpha (p+2q)_\beta}{(p+q)^4 q^2} \\ &\quad \times \left[ \frac{B(l_z)}{|p|} \left( \delta_{\mu\alpha} - \frac{p_\mu p_\alpha}{p^2} \right) - \frac{\epsilon_{\mu\alpha\lambda} p_\lambda}{p^2} \right] \left[ \frac{B(q_z - l_z)}{|p|} \left( \delta_{\mu\beta} - \frac{p_\mu p_\beta}{p^2} \right) + \frac{\epsilon_{\mu\beta\sigma} p_\sigma}{p^2} \right]. \end{aligned} \quad (\text{C.9})$$

478 We calculate the 4 crossing terms one by one. The first term has an integral



Integral 1

$$\begin{aligned}
&= \int \frac{d^3 p}{(2\pi)^3} \frac{d^3 q}{(2\pi)^3} \frac{(p+2q)_\alpha (p+2q)_\beta}{p^2 (p+q)^4 q^2} \cdot \left( \delta_{\mu\alpha} - \frac{p_\mu p_\alpha}{p^2} \right) \left( \delta_{\mu\beta} - \frac{p_\mu p_\beta}{p^2} \right) \\
&= \int \frac{d^3 p}{(2\pi)^3} \frac{d^3 q}{(2\pi)^3} \left( \frac{(p+2q)^2}{p^2 (p+q)^4 q^2} - \frac{(p \cdot (p+2q))^2}{p^4 (p+q)^4 q^2} \right) \\
&= \text{Integral 1.1} - \text{Integral 1.2.}
\end{aligned} \tag{C.10}$$

479 First, we show that Integral 1.2 vanishes:

Integral 1.2

$$\begin{aligned}
&= \int \frac{d^3 p}{(2\pi)^3} \frac{d^3 q}{(2\pi)^3} \frac{(p^2 + 2p \cdot q)^2}{p^4 (p+q)^4 q^2} \\
&= \int \frac{d^3 p}{(2\pi)^3} \frac{d^3 q}{(2\pi)^3} \frac{((p+q)^2 - q^2)^2}{p^4 (p+q)^4 q^2} \\
&= \int \frac{d^3 p}{(2\pi)^3} \frac{d^3 q}{(2\pi)^3} \left( \frac{1}{p^4 q^2} + \frac{q^2}{p^4 (p+q)^4} - \frac{2}{p^4 (p+q)^2} \right) \\
&= \int \frac{d^3 p}{(2\pi)^3} \frac{d^3 q}{(2\pi)^3} \left( \frac{1}{p^4 q^2} + \frac{(q-p)^2}{p^4 q^4} - \frac{2}{p^4 q^2} \right) \\
&= \int \frac{d^3 p}{(2\pi)^3} \frac{d^3 q}{(2\pi)^3} \left( -\frac{2p \cdot q}{p^4 q^2} + \frac{1}{p^2 q^4} \right) \\
&= 0.
\end{aligned} \tag{C.11}$$

480 In the intermediate steps we shifted the integral variables. Then we calculate Integral 1.1:

Integral 1.1

$$\begin{aligned}
&= \int \frac{d^3 p}{(2\pi)^3} \frac{d^3 q}{(2\pi)^3} \frac{(p+2q)^2}{p^2 (p+q)^4 q^2} \\
&= \int \frac{d^3 p}{(2\pi)^3} \frac{d^3 q}{(2\pi)^3} \frac{(p+q)^2}{p^4 (p-q)^2 q^2} \\
&= \int \frac{d^3 p}{(2\pi)^3} \frac{d^3 q}{(2\pi)^3} \frac{(p-q)^2 + 4p \cdot q}{p^4 (p-q)^2 q^2} \\
&= \int \frac{d^3 p}{(2\pi)^3} \frac{d^3 q}{(2\pi)^3} \frac{4p \cdot q}{p^4 (p-q)^2 q^2}.
\end{aligned} \tag{C.12}$$

481 Here we use some useful identities below, which can be derived with the help of Feynman  
482 parametrization:

$$\int \frac{d^3 q}{(2\pi)^3} \frac{1}{q^2 (q+p)^2} = \frac{1}{8|p|}, \tag{C.13}$$

$$\int \frac{d^3 q}{(2\pi)^3} \frac{q_\mu}{q^4 (q+p)^2} = -\frac{p_\mu}{16|p|^3}. \tag{C.14}$$

483 Then

Integral 1.1

$$\begin{aligned}
&= \int \frac{d^3q}{(2\pi)^3} 4q_\mu \int \frac{d^3p}{(2\pi)^3} \frac{p_\mu}{p^4(p-q)^2} \\
&= \int \frac{d^3q}{(2\pi)^3} \frac{4q_\mu}{q^2} \frac{q_\mu}{16|q|^3} \\
&= \int \frac{d^3q}{(2\pi)^3} \frac{1}{4|q|^3} \\
&= \frac{1}{16\pi^2} \ln x^2 \Lambda^2,
\end{aligned} \tag{C.15}$$

484 thus we finish the calculation of the first integral and get

$$\text{Integral 1} = \frac{1}{16\pi^2} \ln x^2 \Lambda^2. \tag{C.16}$$

485 The second and third integral vanish. For example,

$$\text{Integral 2} = \int \frac{d^3p}{(2\pi)^3} \frac{d^3q}{(2\pi)^3} \frac{(p+2q)_\alpha (p+2q)_\beta}{|p|^3 (p+q)^4 q^2} \left( \delta_{\mu\alpha} - \frac{p_\mu p_\alpha}{p^2} \right) \epsilon_{\mu\beta\sigma} p_\sigma = 0 \tag{C.17}$$

486 vanishes due to the anti-symmetric symbol.

487 Finally, we do the fourth integral. Using  $\epsilon_{\mu\alpha\lambda} \epsilon_{\mu\beta\sigma} = \delta_{\alpha\beta} \delta_{\lambda\sigma} - \delta_{\alpha\sigma} \delta_{\lambda\beta}$ ,

Integral 4

$$\begin{aligned}
&= \int \frac{d^3p}{(2\pi)^3} \frac{d^3q}{(2\pi)^3} \frac{-(p+2q)_\alpha (p+2q)_\beta}{p^4 (p+q)^4 q^2} \epsilon_{\mu\alpha\lambda} \epsilon_{\mu\beta\sigma} p_\lambda p_\sigma \\
&= \int \frac{d^3p}{(2\pi)^3} \frac{d^3q}{(2\pi)^3} \frac{(p \cdot (p+2q))^2 - p^2 (p+2q)^2}{p^4 (p+q)^4 q^2} \\
&= \int \frac{d^3p}{(2\pi)^3} \frac{d^3q}{(2\pi)^3} \frac{[(p+q)^2 - q^2]^2 - p^2 (p+2q)^2}{p^4 (p+q)^4 q^2} \\
&= \int \frac{d^3p}{(2\pi)^3} \frac{d^3q}{(2\pi)^3} \frac{(p+q)^4 - 2q^2 (p+q)^2 + q^4 - p^2 (p+2q)^2}{p^4 (p+q)^4 q^2} \\
&= \int \frac{d^3p}{(2\pi)^3} \frac{d^3q}{(2\pi)^3} \left( \frac{1}{p^4 q^2} - \frac{2}{p^4 (p+q)^2} + \frac{q^2}{p^4 (p+q)^4} \right) - \text{Integral 1.1} \\
&= \int \frac{d^3p}{(2\pi)^3} \frac{d^3q}{(2\pi)^3} \left( \frac{1}{p^4 q^2} - \frac{2}{p^4 q^2} + \frac{(q-p)^2}{p^4 q^4} \right) - \text{Integral 1.1} \\
&= -\text{Integral 1.1} = -\frac{1}{16\pi^2} \ln x^2 \Lambda^2.
\end{aligned} \tag{C.18}$$

488 So we have

Graph F(amputated)

$$= -\left( \frac{1}{4\pi|x|} \right)^2 \frac{1}{4\pi^2 N^2} \sum_{q_z, l_z} e^{iq_z \cdot (i-j)} A(l_z) A(q_z - l_z) (B(l_z) B(q_z - l_z) - 1) \ln x^2 \Lambda^2. \tag{C.19}$$

489 Using Eq. C.6, we get the result of Graph F in Table. 2.

## 490 D Electromagnetic response of the iCSM

491 To calculate its electromagnetic response, we couple the physical current with external elec-  
492 tromagnetic field  $A_\mu^z$  by adding the following term to Eq. 57:

$$S_c = -\frac{i}{2\pi} \sum_z \int d^3x \epsilon_{\mu\nu\rho} A_\mu^z \partial_\nu a_\rho^z, \quad (\text{D.1})$$

493 where we assume unit  $U(1)$  charges of the quasiparticle for every layer. Integrating out  $a_\mu$ ,  
494 we get the effective action

$$S_{\text{eff}}[A_\mu] = \frac{1}{2} \sum_{q_z} \int \frac{d^3q}{(2\pi)^3} A_\mu^{q_z}(q) \Pi_{\mu\nu}^{q_z} A_\nu^{-q_z}(-q), \quad (\text{D.2})$$

495 with the response kernel

$$\Pi_{\mu\nu}^{q_z}(q) = \frac{1}{4\pi^2} \frac{\left(\frac{q^2}{g^2} + u(q_z)\right)(q^2 \delta_{\mu\nu} - q_\mu q_\nu)}{C^2 q^2 + \left(\frac{q^2}{g^2} + u(q_z)\right)^2} + \frac{1}{4\pi^2} \frac{C q^2 \epsilon_{\mu\rho\nu} q_\rho}{C^2 q^2 + \left(\frac{q^2}{g^2} + u(q_z)\right)^2}, \quad (\text{D.3})$$

496 where  $C(q_z) = \frac{1}{2\pi}(c_0 + 2c_1 \cos q_z)$ ,  $u(q_z) = 4\rho_s \sin^2 \frac{q_z}{2}$ ,  $\epsilon_{012} = -1$ . The conductivity tensor can  
497 be obtained from this response kernel by the following equation:

$$\sigma_{ij}^{q_z}(\omega) = \frac{-1}{i\omega} \Pi_{ij}^{q_z}(i\omega \rightarrow (\omega + i0^+), \mathbf{q} = 0), \quad (\text{D.4})$$

498 and we get:

$$\begin{aligned} \sigma_{xx}^{q_z}(\omega) &= \frac{1}{4\pi^2} \frac{-i\omega(u(q_z) - \omega^2/g^2)}{(u(q_z) - \omega^2/g^2)^2 - C^2 \omega^2}, \\ \sigma_{xy}^{q_z}(\omega) &= \frac{1}{4\pi^2} \frac{-C \omega^2}{(u(q_z) - \omega^2/g^2)^2 - C^2 \omega^2}. \end{aligned} \quad (\text{D.5})$$

499 Note that both  $\sigma_{xx}$  and  $\sigma_{xy}$  vanish in the DC ( $\omega = 0$ ) limit at finite  $q_z \neq 0$ , like a trivial in-  
500 sulator. Only at  $q_z = 0$ ,  $\sigma_{xx}^{q_z=0}(\omega = 0) = 0$  and  $\sigma_{xy}^{q_z=0}(\omega = 0) = \frac{1}{c_0 + 2c_1} \frac{e^2}{h}$ , like a FQHE insulator.  
501 If we let  $\rho_s = 0$  and take the  $g^2 \rightarrow \infty$  limit, which corresponds to the 2D iCSM, from Eq. D.5 we  
502 get the DC conductivity tensor  $\sigma_{xx}^{q_z}(\omega = 0) = 0$ ,  $\sigma_{xy}^{q_z}(\omega = 0) = \frac{1}{2\pi(c_0 + 2c_1 \cos q_z)} = \frac{1}{c_0 + 2c_1 \cos q_z} \frac{e^2}{h}$ .  
503 By Fourier transforming it into real space, we have the following conductivity tensor for 2D  
504 iCSM:

$$\begin{aligned} \sigma_{xx}^{z-z'}(\omega = 0) &= 0, \\ \sigma_{xy}^{z-z'}(\omega = 0) &= \frac{e^2}{h} (K)_{z,z'}^{-1}. \end{aligned} \quad (\text{D.6})$$

## 505 References

- 506 [1] S. Sachdev, *Quantum phase transitions*, Physics World **12**(4), 33 (1999),  
507 doi:10.1088/2058-7058/12/4/23.
- 508 [2] S. Sondhi, S. Girvin, J. Carini and D. Shahar, *Continuous quantum phase transitions*,  
509 Reviews of Modern Physics **69** (1996), doi:10.1103/RevModPhys.69.315.

- 510 [3] V. Kalmeyer and R. B. Laughlin, *Equivalence of the resonating-valence-*  
511 *bond and fractional quantum hall states*, Phys. Rev. Lett. **59**, 2095 (1987),  
512 doi:[10.1103/PhysRevLett.59.2095](https://doi.org/10.1103/PhysRevLett.59.2095).
- 513 [4] X. G. Wen, F. Wilczek and A. Zee, *Chiral spin states and superconductivity*, Phys. Rev. B  
514 **39**, 11413 (1989), doi:[10.1103/PhysRevB.39.11413](https://doi.org/10.1103/PhysRevB.39.11413).
- 515 [5] B. Bauer, L. Cincio, B. P. Keller, M. Dolfi, G. Vidal, S. Trebst and A. W. W. Ludwig, *Chiral*  
516 *spin liquid and emergent anyons in a Kagome lattice Mott insulator*, Nature Communica-  
517 tions **5**, 5137 (2014), doi:[10.1038/ncomms6137](https://doi.org/10.1038/ncomms6137), [1401.3017](https://doi.org/10.1038/ncomms6137).
- 518 [6] Y.-C. He, D. N. Sheng and Y. Chen, *Chiral Spin Liquid in a Frustrated*  
519 *Anisotropic Kagome Heisenberg Model*, Phys. Rev. Lett. **112**(13), 137202 (2014),  
520 doi:[10.1103/PhysRevLett.112.137202](https://doi.org/10.1103/PhysRevLett.112.137202), [1312.3461](https://arxiv.org/abs/1312.3461).
- 521 [7] S.-S. Gong, W. Zhu and D. N. Sheng, *Emergent Chiral Spin Liquid: Fractional Quan-*  
522 *tum Hall Effect in a Kagome Heisenberg Model*, Scientific Reports **4**, 6317 (2014),  
523 doi:[10.1038/srep06317](https://doi.org/10.1038/srep06317), [1312.4519](https://arxiv.org/abs/1312.4519).
- 524 [8] Y.-C. He and Y. Chen, *Distinct Spin Liquids and Their Transitions in Spin-1*  
525 */2 X X Z Kagome Antiferromagnets*, Phys. Rev. Lett. **114**(3), 037201 (2015),  
526 doi:[10.1103/PhysRevLett.114.037201](https://doi.org/10.1103/PhysRevLett.114.037201), [1407.2740](https://arxiv.org/abs/1407.2740).
- 527 [9] A. Szasz, J. Motruk, M. P. Zaletel and J. E. Moore, *Chiral Spin Liquid Phase of the Tri-*  
528 *angular Lattice Hubbard Model: A Density Matrix Renormalization Group Study*, Physical  
529 Review X **10**(2), 021042 (2020), doi:[10.1103/PhysRevX.10.021042](https://doi.org/10.1103/PhysRevX.10.021042).
- 530 [10] W.-J. Hu, S.-S. Gong and D. N. Sheng, *Variational Monte Carlo study of chiral spin liquid*  
531 *in quantum antiferromagnet on the triangular lattice*, Phys. Rev. B **94**(7), 075131 (2016),  
532 doi:[10.1103/PhysRevB.94.075131](https://doi.org/10.1103/PhysRevB.94.075131), [1603.03365](https://arxiv.org/abs/1603.03365).
- 533 [11] A. Wietek, A. Sterdyniak and A. M. Läuchli, *Nature of chiral spin liquids on the kagome*  
534 *lattice*, Phys. Rev. B **92**, 125122 (2015), doi:[10.1103/PhysRevB.92.125122](https://doi.org/10.1103/PhysRevB.92.125122).
- 535 [12] N. Y. Yao, M. P. Zaletel, D. M. Stamper-Kurn and A. Vishwanath, *A quantum dipolar spin*  
536 *liquid*, Nature Physics **14**(4), 405–410 (2018), doi:[10.1038/s41567-017-0030-7](https://doi.org/10.1038/s41567-017-0030-7).
- 537 [13] A. Wietek, R. Rossi, F. S. IV, M. Klett, P. Hansmann, M. Ferrero, E. M. Stoudenmire,  
538 T. Schafer and A. Georges, *Mott insulating states with competing orders in the triangular*  
539 *lattice hubbard model* (2021), [2102.12904](https://arxiv.org/abs/2102.12904).
- 540 [14] A. Szasz and J. Motruk, *Phase diagram of the anisotropic triangular lattice hubbard model*  
541 (2021), [2101.07454](https://arxiv.org/abs/2101.07454).
- 542 [15] Z. Zhu, D. N. Sheng and A. Vishwanath, *Doped mott insulators in the triangular-lattice*  
543 *hubbard model*, Phys. Rev. B **105**, 205110 (2022), doi:[10.1103/PhysRevB.105.205110](https://doi.org/10.1103/PhysRevB.105.205110).
- 544 [16] B.-B. Chen, Z. Chen, S.-S. Gong, D. N. Sheng, W. Li and A. Weichselbaum, *Quantum spin*  
545 *liquid with emergent chiral order in the triangular-lattice hubbard model* (2021), [2102.](https://arxiv.org/abs/2102.05560)  
546 [05560](https://arxiv.org/abs/2102.05560).
- 547 [17] C. Hickey, L. Cincio, Z. Papić and A. Paramekanti, *Emergence of chiral spin liquids via*  
548 *quantum melting of noncoplanar magnetic orders*, Phys. Rev. B **96**, 115115 (2017),  
549 doi:[10.1103/PhysRevB.96.115115](https://doi.org/10.1103/PhysRevB.96.115115).

- 550 [18] M. Hermele, V. Gurarie and A. M. Rey, *Mott insulators of ultracold fermionic alkaline earth*  
551 *atoms: Underconstrained magnetism and chiral spin liquid*, Phys. Rev. Lett. **103**, 135301  
552 (2009), doi:[10.1103/PhysRevLett.103.135301](https://doi.org/10.1103/PhysRevLett.103.135301).
- 553 [19] P. Nataf, M. Lajkó, A. Wietek, K. Penc, F. Mila and A. M. Läuchli, *Chiral spin liquids in*  
554 *triangular-lattice SU(n) fermionic mott insulators with artificial gauge fields*, Phys. Rev.  
555 Lett. **117**, 167202 (2016), doi:[10.1103/PhysRevLett.117.167202](https://doi.org/10.1103/PhysRevLett.117.167202).
- 556 [20] J.-Y. Chen, S. Capponi, A. Wietek, M. Mambrini, N. Schuch and D. Poilblanc, *SU(3)<sub>1</sub>*  
557 *chiral spin liquid on the square lattice: A view from symmetric projected entangled pair*  
558 *states*, Phys. Rev. Lett. **125**, 017201 (2020), doi:[10.1103/PhysRevLett.125.017201](https://doi.org/10.1103/PhysRevLett.125.017201).
- 559 [21] C. Boos, C. J. Ganahl, M. Lajkó, P. Nataf, A. M. Läuchli, K. Penc, K. P. Schmidt and  
560 F. Mila, *Time-reversal symmetry breaking abelian chiral spin liquid in mott phases of*  
561 *three-component fermions on the triangular lattice*, Phys. Rev. Res. **2**, 023098 (2020),  
562 doi:[10.1103/PhysRevResearch.2.023098](https://doi.org/10.1103/PhysRevResearch.2.023098).
- 563 [22] X.-P. Yao, Y. Gao and G. Chen, *Topological chiral spin liquids and competing states*  
564 *in triangular lattice SU(n) mott insulators*, Phys. Rev. Res. **3**, 023138 (2021),  
565 doi:[10.1103/PhysRevResearch.3.023138](https://doi.org/10.1103/PhysRevResearch.3.023138).
- 566 [23] Y.-H. Wu and H.-H. Tu, *Possible su(3) chiral spin liquid on the kagome lattice*, Phys. Rev.  
567 B **94**, 201113 (2016), doi:[10.1103/PhysRevB.94.201113](https://doi.org/10.1103/PhysRevB.94.201113).
- 568 [24] H.-H. Tu, A. E. Nielsen and G. Sierra, *Quantum spin models for the*  
569 *su(n)<sub>1</sub> wess–zumino–witten model*, Nuclear Physics B **886**, 328 (2014),  
570 doi:<https://doi.org/10.1016/j.nuclphysb.2014.06.027>.
- 571 [25] Y.-H. Zhang, D. N. Sheng and A. Vishwanath, *Su(4) chiral spin liquid, exciton super-*  
572 *solid, and electric detection in moiré bilayers*, Phys. Rev. Lett. **127**, 247701 (2021),  
573 doi:[10.1103/PhysRevLett.127.247701](https://doi.org/10.1103/PhysRevLett.127.247701).
- 574 [26] R. B. Laughlin, *Quantized hall conductivity in two dimensions*, Phys. Rev. B **23**, 5632  
575 (1981), doi:[10.1103/PhysRevB.23.5632](https://doi.org/10.1103/PhysRevB.23.5632).
- 576 [27] X.-G. Wen, *Quantum field theory of many-body systems: From the origin of sound*  
577 *to an origin of light and electrons*, Quantum Field Theory of Many-Body Systems:  
578 From the Origin of Sound to an Origin of Light and Electrons pp. 1–520 (2010),  
579 doi:[10.1093/acprof:oso/9780199227259.001.0001](https://doi.org/10.1093/acprof:oso/9780199227259.001.0001).
- 580 [28] M. Levin and M. P. A. Fisher, *Gapless layered three-dimensional fractional quantum hall*  
581 *states*, Phys. Rev. B **79**, 235315 (2009), doi:[10.1103/PhysRevB.79.235315](https://doi.org/10.1103/PhysRevB.79.235315).
- 582 [29] X. Ma, W. Shirley, M. Cheng, M. Levin, J. McGreevy and X. Chen, *Fractonic order*  
583 *in infinite-component chern-simons gauge theories*, Phys. Rev. B **105**, 195124 (2022),  
584 doi:[10.1103/PhysRevB.105.195124](https://doi.org/10.1103/PhysRevB.105.195124).
- 585 [30] J. Sullivan, A. Dua and M. Cheng, *Weak symmetry breaking and topological order in a 3d*  
586 *compressible quantum liquid* (2021), [2109.13267](https://arxiv.org/abs/2109.13267).
- 587 [31] X. Chen, H. T. Lam and X. Ma, *Gapless infinite-component chern-simons-maxwell theories*  
588 (2022), [2211.10458](https://arxiv.org/abs/2211.10458).
- 589 [32] M. Pretko, X. Chen and Y. You, *Fracton phases of matter*, International Journal of Modern  
590 Physics A **35**(06), 2030003 (2020), doi:[10.1142/s0217751x20300033](https://doi.org/10.1142/s0217751x20300033).

- 591 [33] R. M. Nandkishore and M. Hermele, *Fractons*, Annual Review of Condensed Matter  
592 Physics **10**(1), 295 (2019), doi:[10.1146/annurev-conmatphys-031218-013604](https://doi.org/10.1146/annurev-conmatphys-031218-013604), <https://doi.org/10.1146/annurev-conmatphys-031218-013604>.  
593
- 594 [34] E. Lake and M. Hermele, *Subdimensional criticality: Condensation of li-*  
595 *neons and planons in the x-cube model*, Phys. Rev. B **104**, 165121 (2021),  
596 doi:[10.1103/PhysRevB.104.165121](https://doi.org/10.1103/PhysRevB.104.165121).
- 597 [35] A. Altland and B. D. Simons, *Condensed Matter Field Theory*, Cambridge University Press,  
598 2 edn., doi:[10.1017/CBO9780511789984](https://doi.org/10.1017/CBO9780511789984) (2010).
- 599 [36] S. Benvenuti and H. Khachatryan, *Easy-plane qed3's in the large nf limit*, Journal of High  
600 Energy Physics **2019**(5), 214 (2019), doi:[10.1007/JHEP05\(2019\)214](https://doi.org/10.1007/JHEP05(2019)214).
- 601 [37] G. W. Semenoff, P. Sodano and Y.-S. Wu, *Renormalization of the statistics pa-*  
602 *rameter in three-dimensional electrodynamics*, Phys. Rev. Lett. **62**, 715 (1989),  
603 doi:[10.1103/PhysRevLett.62.715](https://doi.org/10.1103/PhysRevLett.62.715).
- 604 [38] W. Chen, M. P. A. Fisher and Y.-S. Wu, *Mott transition in an anyon gas*, Phys. Rev. B **48**,  
605 13749 (1993), doi:[10.1103/PhysRevB.48.13749](https://doi.org/10.1103/PhysRevB.48.13749).
- 606 [39] L. Zou and T. Senthil, *Dimensional decoupling at continuous quantum critical mott transi-*  
607 *tions*, Phys. Rev. B **94**, 115113 (2016), doi:[10.1103/PhysRevB.94.115113](https://doi.org/10.1103/PhysRevB.94.115113).